NAVAL POSTGRADUATE SCHOOL

MONTEREY, CALIFORNIA

THESIS

INVESTIGATIONS OF PARAMETRIC EXCITATION IN PHYSICAL SYSTEMS

by

Michael T. Janssen

June 2005

Thesis Advisor:	Bruce C. Denardo
Co-Advisor:	Thomas Hofler

Approved for public release; distribution is unlimited

THIS PAGE INTENTIONALLY LEFT BLANK

REPORT DOCUMENTATION PAGE		Form Approved OMB No. 0704-0188
Public reporting burden for this collection of information is estimated to average 1 hour per response, including the time for reviewing instruction, searching existing data sources, gathering and maintaining the data needed, and completing and reviewing the collection of information. Send comments regarding this burden estimate or any other aspect of this collection of information, including suggestions for reducing this burden, to Washington headquarters Services, Directorate for Information Operations and Reports, 1215 Jefferson Davis Highway, Suite 1204, Arlington, VA 22202-4302, and to the Office of Management and Budget, Paperwork Reduction Project (0704-0188) Washington DC 20503.		
1. AGENCY USE ONLY ***(Leave blank)***	**2. REPORT DATE** June 2005	**3. REPORT TYPE AND DATES COVERED** Master's Thesis
4. TITLE AND SUBTITLE: Investigations of Parametric Excitation in Physical Systems		**5. FUNDING NUMBERS**
6. AUTHOR(S) Michael T Janssen		
7. PERFORMING ORGANIZATION NAME(S) AND ADDRESS(ES) Naval Postgraduate School Monterey, CA 93943-5000		**8. PERFORMING ORGANIZATION REPORT NUMBER**
9. SPONSORING /MONITORING AGENCY NAME(S) AND ADDRESS(ES) N/A		**10. SPONSORING/MONITORING AGENCY REPORT NUMBER** N/A
11. SUPPLEMENTARY NOTES The views expressed in this thesis are those of the author and do not reflect the official policy or position of the Department of Defense or the U.S. Government.		
12a. DISTRIBUTION / AVAILABILITY STATEMENT Approved for public release; distribution is unlimited.		**12b. DISTRIBUTION CODE**

13. ABSTRACT (maximum 200 words)

Parametric excitation can occur when the value of a parameter of an oscillator is modulated at twice the natural frequency of the oscillator. The response grows exponentially and is only limited by a nonlinearity of the system, so large response amplitudes typically occur. However, there is no response unless the parametric drive amplitude is above a threshold value that is dictated by the damping. We investigate parametric excitation in three physical systems. The first involves an acoustic standing wave in a pipe that is driven by a piston at one end. An analysis shows that parametric excitation is not feasible in this system unless one uses a very large-excursion piston (for example, from an aircraft engine). The second system is an inductor-capacitor circuit which can undergo oscillations of the current. An analysis of capacitance modulation with a bank of alternate rotating and stationary parallel plates shows that parametric excitation would be very difficult to achieve. Finally, we describe the construction of a torsional oscillator whose length is modulated. Parametric excitation is successfully demonstrated in this system. A comparison of data to predictions of the standard theory of parametric excitation reveals significant deviations.

14. SUBJECT TERMS Parametric excitation, torsional oscillator, capacitance modulation, and length modulation.			**15. NUMBER OF PAGES** 79
			16. PRICE CODE
17.SECURITY CLASSIFICATION OF REPORT Unclassified	**18.SECURITY CLASSIFICATION OF THIS PAGE** Unclassified	**19.SECURITY CLASSIFICATION OF ABSTRACT** Unclassified	**20. LIMITATION OF ABSTRACT** UL

NSN 7540-01-280-5500

Standard Form 298 (Rev. 2-89)
Prescribed by ANSI Std. 239-18

THIS PAGE INTENTIONALLY LEFT BLANK

Approved for public release; distribution is unlimited

INVESTIGATIONS OF PARAMETRIC EXCITATION IN PHYSICAL SYSTEMS

Michael T. Janssen
Ensign, United States Navy
B.S., Rensselaer Polytechnic Institute, 2004

Submitted in partial fulfillment of the
requirements for the degree of

MASTER OF SCIENCE IN ENGINEERING ACOUSTICS

from the

NAVAL POSTGRADUATE SCHOOL
June 2005

Author: Michael T. Janssen

Approved by: Bruce C. Denardo
Thesis Advisor

Thomas Holfer
Thesis Co-Advisor

Kevin Smith
Chair, Engineering Acoustics Academic Committee

THIS PAGE INTENTIONALLY LEFT BLANK

ABSTRACT

Parametric excitation can occur when the value of a parameter of an oscillator is modulated at twice the natural frequency of the oscillator. The response grows exponentially and is only limited by a nonlinearity of the system, so large response amplitudes typically occur. However, there is no response unless the parametric drive amplitude is above a threshold value that is dictated by the damping. We investigate parametric excitation in three physical systems. The first involves an acoustic standing wave in a pipe that is driven by a piston at one end. An analysis shows that parametric excitation is not feasible in this system unless one uses a very large-excursion piston (for example, from an aircraft engine). The second system is an inductor-capacitor circuit which can undergo oscillations of the current. An analysis of capacitance modulation with a bank of alternate rotating and stationary parallel plates shows that parametric excitation would be very difficult to achieve. Finally, we describe the construction of a torsional oscillator whose length is modulated. Parametric excitation is successfully demonstrated in this system. A comparison of data to predictions of the standard theory of parametric excitation reveals significant deviations.

THIS PAGE INTENTIONALLY LEFT BLANK

TABLE OF CONTENTS

THIS PAGE INTENTIONALLY LEFT BLANK

LIST OF FIGURES

LIST OF TABLES

THIS PAGE INTENTIONALLY LEFT BLANK

LIST OF SYMBOLS

a	radius
A	amplitude, or area
C_{max}	maximum capacitance
C_0	ambient capacitance
C_{th}	threshold capacitance
ΔC	change in capacitance
d	distance between plates
D	plate diameter
E	energy
f_{mod}	frequency of modulation
f_0	natural frequency
f_{rot}	frequency of rotation
h	plate thickness
L	inductance or length
L_{th}	threshold length
n	number of plates
N	number of sectors cut out of plate
P	power
Pr	Prandtl number
Q	overall quality factor
Q_{rad}	quality factor due to radiation losses
Q_{visc}	quality factor due to viscous losses
Q_{therm}	quality factor due to thermal losses
r	plate radius
R	resistance
t	time
x	displacement from equilibrium

α	nonlinear coefficient
β	linear damping coefficient
δ_{therm}	thermal penetration depth
δ_{visc}	viscous penetration depth
ε_0	electric permittivity constant
η	shear viscosity
I	moment of inertia
λ	wavelength
κ	torsional constant
π	pi, constant 3.1416
γ	ratio of specific heats
ρ	density
τ	torque
θ	angular displacement from equilibrium
T	ramp-up time
ω	angular acceleration or frequency

ACKNOWLEDGEMENTS

I would be incredible remiss if I did not thank my wife first. She has been more supportive then I could ever ask, both now and always. She has endured the busy nights, and the long days. She never complained and always greeted me with a smile and a kiss when ever I came home, no matter what hour. To you Tiffany I will always be grateful. To my son Brynan, you taught me that playtime is *very* important and not to forget it. To my daughter Katelynne, you showed me that good things do come in small packages, and to keep it simple.

I would also like to extend my gratitude to Professor Denardo. I know that at time I was frustrating, but for me it was all a learning process and I appreciate your patience. I also want to thank you for the classes you taught, it is clear that you care about your students.

To LT Lindberg, LT Sundem, and ENS Jones, thanks for the much need stress relief.

Finally, I would like to thank God. Some would say that science and religion do not go together. I believe in both and I do not think that they can be separated.

THIS PAGE INTENTIONALLY LEFT BLANK

I. INTRODUCTION

The basic theoretical features of parametric excitation and other important background material is presented in Sec. A. Motivations and objectives of this thesis are explained in Sec. B.

A. PARAMETRIC EXCITATION

A linearly-damped oscillator is described by

$$\frac{d^2x}{dt^2} + 2\beta\frac{dx}{dt} + \omega_0^2 x = 0 , \qquad (1. .1)$$

where x(t) is the displacement of the mass from equilibrium, β is the damping parameter, and ω_0 is the natural frequency of the oscillator. The behavior of this oscillator is exponentially-damped simple harmonic motion:

$$x(t) = Ae^{-\beta t}\cos(\omega_0 t - \delta) , \qquad (1.A.1)$$

where the values of the amplitude A and phase δ depend upon initial conditions. That the amplitude decays exponentially with decay constant β offers a means of experimentally determining β for an oscillator.

There are three types of driving mechanisms that can excite and maintain the motion of an oscillator: (i) direct, (ii) maintained, and (iii) parametric. The mathematically simplest case is (i), where an oscillatory force is exerted on the mass of the oscillator. An inhomogeneous term is thus added to the equation of motion (1.A.1). Case (ii) is the most common (for example, voice, whistling, and woodwind musical instruments), although this case is mathematically the most difficult. The drive is typically described as a negative damping term in the

equation of motion (1.A.1). It is the derivation of this term for any specific physical system that is typically difficult.

Case (iii) is the subject of this thesis. *Parametric excitation* occurs when an external agent modulates a parameter upon which the natural frequency of an oscillator depends. The standard equation of motion is the linearly-damped *Mathieu equation*:

$$\frac{d^2x}{dt^2} + 2\beta\frac{dx}{dt} + \omega_0^2\left[1+\eta\cos(\omega t)\right]x = 0 , \qquad (1.A.2)$$

where η is the *dimensionless parametric drive amplitude* and ω is the *parametric drive frequency*. Note that the parametric drive is represented by a homogeneous term in the equation of motion (1.A.3). We will deal with the *principal* parametric resonance, which occurs when ω is near $2\omega_0$. It can be shown that a parametric drive causes an exponential growth of the response (Denardo and Larraza, 2004), and thus competes with the exponential decay caused by linear damping. Hence, if η exceeds the *parametric drive threshold*, the response grows without limit in the linear case (1.A.3). For weak damping, weak parametric drive, and ω near $2\omega_0$, the threshold curve due to Eq. (1.A.3) is

$$\eta_{th}^2 = \frac{4}{\omega_0^2}\left[(\omega - 2\omega_0)^2 + 4\beta^2\right] , \qquad (1.A.3)$$

which is an hyperbola in the drive plane of η vs. ω (Denardo and Larraza, 2004). Parametric excitation occurs if $\eta > \eta_{th}$. The minimum drive threshold corresponds to $\omega = 2\omega_0$ and has the value

$$(\eta_{th})_{min} = \frac{2}{Q} , \qquad (1.A.4)$$

where the quality factor of the oscillator is

$$Q = \frac{\omega_0}{2\beta} . \qquad (1.A.5)$$

If excitation occurs, the response grows without bound. Because the response of any actual oscillator cannot be infinite, it is guaranteed that nonlinearity must emerge to limit the growth. We add a cubic nonlinearity in the displacement to Eq. (1.A.3), because this nonlinearity is the simplest, and because it corresponds to an oscillator with a symmetric potential energy, which models the case of a length-modulated torsional oscillator (Ch. IV). The equation of motion is thus

$$\frac{d^2x}{dt^2} + 2\beta\frac{dx}{dt} + \omega_0^2\left[1+\eta\cos(\omega t)\right]x = \alpha x^3 , \qquad (1.A.6)$$

where the *nonlinear coefficient* α can be positive or negative.

The nonlinear coefficient describes how the frequency of undamped undriven oscillations depends upon amplitude. For $\beta = \eta = 0$ in Eq. (1.A.7), we set $x = A\cos(\omega t)$ + {higher harmonics}, where ω is the response frequency, and where the amplitudes of the higher harmonics are small compared to A for weakly nonlinear motion. Solving approximately for ω then yields (Denardo and Larraza, 2004)

$$\omega = \omega_0 - \frac{3\alpha}{8\omega_0}A^2 . \qquad (1.A.7)$$

The oscillations *soften* for $\alpha > 0$ and *harden* for $\alpha < 0$. For the purposes of dealing with damped driven response curves of steady-state motion, it is convenient to view Eq. (1.A.8) as yielding the *backbone* curve of A vs. ω. The natural linear frequency ω_0 can be experimentally determined as the abscissa (A

= 0) intercept of the backbone curve. That A^2 vs. ω is a straight line with slope = $8\omega_0/(3\alpha)$ then offers a means of experimentally determining the nonlinear coefficient α.

For weak damping, weak drive, and weak nonlinearity, the steady-state response solution of the equation of motion (1.A.8) is (Denardo and Larraza, 2004)

$$A^2 = \frac{4\omega_0}{3\alpha}\left(2\omega_0 - \omega \pm 2\sqrt{\eta^2\omega_0^2 - 16\beta^2}\right) . \qquad (1.A.8)$$

The upper branch ($+\sqrt{}$ for $\alpha > 0$ and $-\sqrt{}$ for $\alpha < 0$) is stable, and the lower branch is unstable.

B. MOTIVATIONS AND OBJECTIVES

The original goal of this thesis research was to build an acoustical resonator to observe parametric excitation of a mode. The previous thesis research of Varnadore (2001) and Smith (2003) suggested that the minimum threshold value (1.A.5) could be readily exceeded by a piston-driven pipe. Such an experiment would be important because it could lead to the use of parametric drives in acoustic compressors, pumps, and refrigerators, which require high-amplitude standing waves in order to operate. These devices are of commercial and naval interest because they have very few moving parts and are environmentally friendly.

In Ch. II, we present a detailed feasibility analysis of acoustical parametric excitation by length-modulation of a piston-driven pipe. Our conclusion is that the construction of such an apparatus that would exceed the minimum threshold value (1.A.5) presents a serious engineering challenge involving high-speed long-stroke-length pistons of large area. We thus decided to relegate the experiment to possible future research.

We next examined the feasibility of an inductor-capacitor (LC) circuit in which the capacitance is modulated. An LC circuit oscillates analogously to a mechanical oscillator. Because the frequency depends upon the capacitance, a sufficiently large modulation of the capacitance at twice the natural frequency of the circuit should lead to parametric excitation. Our motivation to build such an apparatus was two-fold. First, the apparatus would be interesting and useful as a demonstration of parametric excitation. The demonstration would be performed in various classes at NPS and elsewhere, and would be especially important for the NPS course PH4459 (Nonlinear Oscillations and Waves). A textbook for this course is currently being written by NPS Profs. Denardo and Larraza (2004). Second, as we explain in Ch. III, there is in the literature only one report of the achievement of parametric excitation by capacitance-modulation of an LC circuit, and this report substantially fails to give sufficient information so that the results can be reproduced. The importance of the experiment is evidenced by its mention in books on nonlinear oscillations. Our second objective was thus to properly perform and report an experiment. However, a detailed feasibility analysis in Ch. III shows that the construction of such an apparatus would again present a serious engineering challenge.

We then turned our attention to a simpler parametric excitation apparatus, although one that does not appear to have been reported in the literature. This system is a torsional oscillator in which a double-roller assembly modulates the length of a twisting strip, and thus modulates the natural frequency of the oscillator. One motivation for constructing this oscillator is its use as a demonstration, as explained above in the case of the LC circuit. Another motivation, as we report in Ch. IV, is that the system is interesting as a case that is well beyond the standard perturbative theory that is used to describe parametric excitation. As described in Ch. IV, we successfully built and tested an apparatus.

THIS PAGE INTENTIONALLY LEFT BLANK

II. PISTON-DRIVEN PIPE

In this chapter, we discuss the theory and feasibility of parametric excitation of an open-ended piston-driven pipe apparatus. In the design, we must ensure that the stroke of the piston drive exceeds the parametric threshold condition (I.A.5), which is $\Delta L_{th}/L = 1/Q$, where ΔL is the peak displacement amplitude of the length of the pipe, L is the ambient length, and Q is the quality factor of the acoustic mode. The quality factor is a result of viscous, thermal, and radiation losses. We first calculate the individual quality factors, from which we determine the overall quality factor and the parametric drive threshold. We then present parametric threshold curves that allow us to choose parameters that optimize the performance of the apparatus. Next, we discuss the feasibility of constructing an apparatus. Our conclusion is that this is possible but extremely difficult.

A. PARAMETRIC DRIVE THRESHOLD

The viscous penetration depth for oscillatory flow near a boundary is (Kinsler et al., 2000)

$$\delta_{visc} = \sqrt{\frac{2\eta}{\rho\omega}} , \qquad (2.A.1)$$

where ρ is the ambient density, η is the shear viscosity, and ω is the angular frequency of the mode. For standing waves in a pipe of radius a, where $\delta_{visc} << a$, the quality factor due to viscous losses is $Q_{visc} = a/\delta_{visc}$, so

$$Q_{visc} = a\sqrt{\frac{\rho\omega}{2\eta}} . \qquad (2.A.2)$$

The thermal penetration depth is (Kinsler et al., 2000)

$$\delta_{therm} = \sqrt{\frac{2\kappa}{c_p \rho \omega}}, \tag{2.A.3}$$

where κ is the thermal conductivity and c_p is the specific heat at constant pressure. The quality factor due to viscous losses is $Q_{therm} = a/[\delta_{therm}(\gamma - 1)]$, where γ is the ratio of specific heats c_p/c_v. Furthermore, the thermal and viscous penetration depths are related by $\delta_{visc}/\delta_{therm} = (Pr)^{1/2}$, where Pr is the Prandtl number. We thus find that the quality factor due to thermal losses is

$$Q_{therm} = a\sqrt{\frac{\rho\omega}{2\eta}}\frac{\sqrt{Pr}}{\gamma - 1} . \tag{2.A.4}$$

When the wavelength of the radiation from an open end of a pipe is much larger than the radius of the pipe, the quality factor due to the radiation is (Kinsler et al., 2000)

$$Q_{rad} = \frac{L\lambda}{A} , \tag{2.A.5}$$

where L is the length of the pipe, λ is the wavelength of the acoustic field, and A is the cross-sectional area of the pipe. Substituting $\lambda = c/f = 2\pi c/\omega$ and $A = \pi a^2$ into Eq. (2.A.5) yields

$$Q_{rad} = \frac{2cL}{a^2\omega} . \tag{2.A.6}$$

As long as a quality factor is not small (specifically, of the order of unity or less), the quality factor is given by 2π times the energy E of the mode divided by the energy loss ΔE per cycle:

$$Q = 2\pi\frac{E}{\Delta E} . \tag{2.A.7}$$

If more than one source of dissipation is present, the energy loss is the sum of the individual energy losses. The quality factors thus add *reciprocally*, so the overall quality factor Q in our case is given by

$$\frac{1}{Q} = \frac{1}{Q_{visc}} + \frac{1}{Q_{therm}} + \frac{1}{Q_{rad}} . \qquad (2.A.8)$$

The parametric threshold condition $\Delta L_{th}/L = 1/Q$ is thus

$$\frac{\Delta L_{th}}{L} = \frac{1}{Q_{visc}} + \frac{1}{Q_{therm}} + \frac{1}{Q_{rad}} . \qquad (2.A.9)$$

Substitution of the expressions (2.A.2), (2.A.4), and (2.A.6) for the individual quality factors yields

$$\Delta L_{th} = \frac{L}{a}\sqrt{\frac{2\eta}{\rho\omega}}\left(1 + \frac{\gamma - 1}{\sqrt{Pr}}\right) + \frac{a^2\omega}{2c} . \qquad (2.A.10)$$

We utilize the following convenient parameters. The diameter is twice the radius: $D = 2a$. The threshold stroke of the piston is twice the peak threshold displacement: $S_{th} = 2\Delta L_{th}$. The parametric drive frequency is twice the natural frequency of the mode: $f_d = 2f_n$, where the natural frequency of the n^{th} mode is approximately $f_n = (2n - 1)c/4L$. These frequency values can be improved by including the effective length due to the opening, and the adjusted speed of sound due to the thermoviscous boundary layer (Kinsler et al., 2000). The approximate effective length for an unflanged opening is $L + 0.6a$. The adjusted speed of sound is

$$c_{adj} = c\left(1 - \frac{\delta_{visc} + \delta_{therm}}{2a}\right) . \qquad (2.A.11)$$

However, because $\delta_{visc} << a$ and $\delta_{therm} << a$ in our case, we take $c_{adj} = c$. The natural frequency of the n^{th} mode is thus

$$f_n = \frac{(2n-1)c}{4(L+0.6a)} . \qquad (2.A.12)$$

where n = 1, 2, 3, …. The parametric drive frequency is twice the modal frequency:

$$f_d = \frac{(2n-1)c}{2(L+0.3D)} , \qquad (2.A.13)$$

where we have also substituted D = 2a. The threshold condition (2.A.10) becomes

$$S_{th} = \frac{4L}{D}\sqrt{\frac{2\eta}{\pi\rho f_d}}\left(1 + \frac{\gamma-1}{\sqrt{Pr}}\right) + \frac{\pi D^2 f_d}{4c} , \qquad (2.A.14)$$

where the drive frequency f_d is given by Eq. (2.A.13). We will deal only with the fundamental (n = 1) mode, so the drive frequency is

$$f_d = \frac{c}{2(L+0.3D)} . \qquad (2.A.15)$$

For the feasibility analysis (next section), we neglect the relatively small end correction term 0.3D in the drive frequency expression (2.A.15), so $f_d = c/2L$. The threshold stroke length thus becomes

$$S_{th} = \frac{8L}{D}\sqrt{\frac{\eta L}{\pi\rho c}}\left(1 + \frac{\gamma-1}{\sqrt{Pr}}\right) + \frac{\pi D^2}{8L} . \qquad (2.A.16)$$

B. INITIAL DESIGN CONCEPT

From the theory we can look at the factors over which we have control and then optimize our system design based on our

choices. The factors are stroke length and piston size. Figure (1) shows the needed stroke length to achieve threshold at different frequencies for different piston sizes.

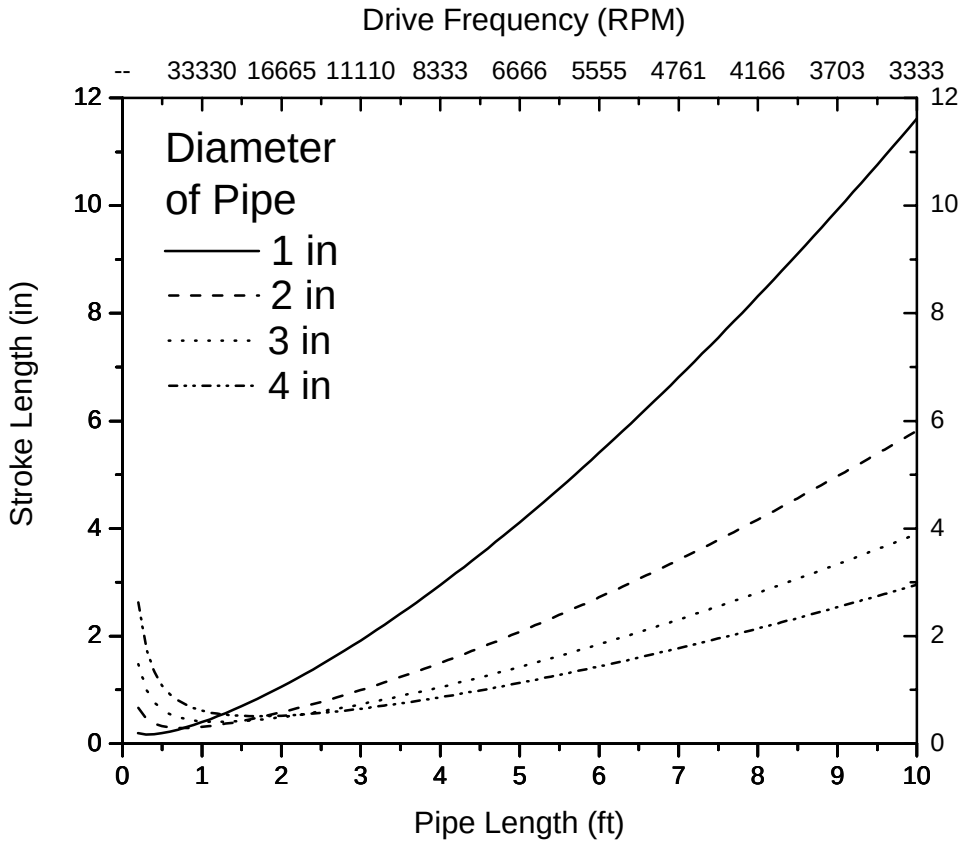

Figure 1. Threshold graph. This graph shows the relationship between drive frequency and the stroke length required to achieve threshold. Different piston diameters are considered.

It is clear from the graph that the higher the drive frequency the lower the required drive amplitude is. For all practical purposes, most pistons will only operate at less than 6000 RPM. On the other hand if the size of the piston is increase, the required drive amplitude is decreased. To be well above threshold and to be at a low enough RPM, would require a very large piston. Though this is not entirely impossible, for the scope of this thesis it is impractical. However,

previous work had lead me to believe that this system might work, so I proceeded with the design process.

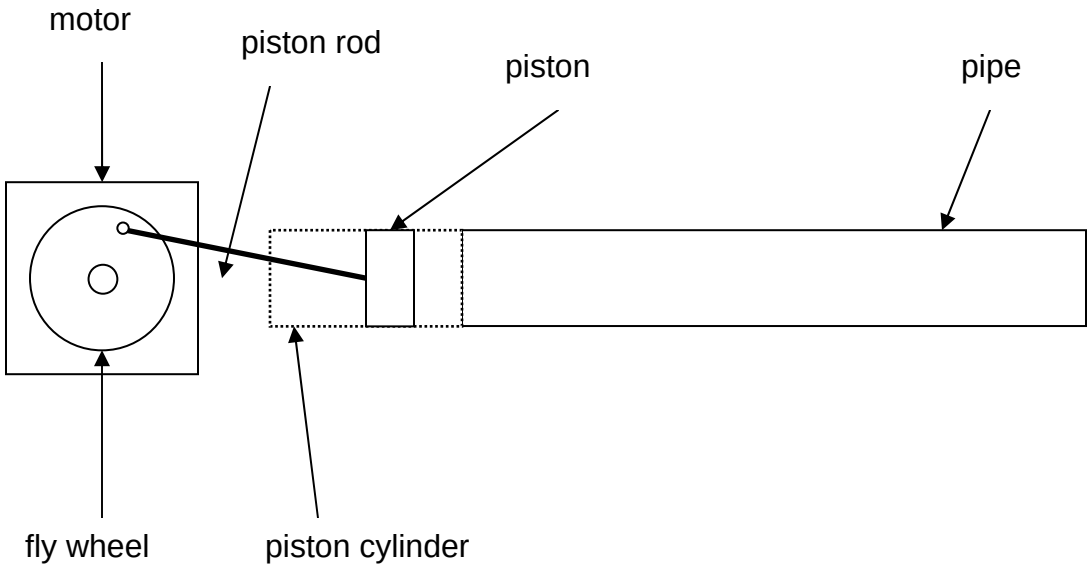

Figure 2. Rendition of initial design concept for parametric acoustic standing wave generator.

Figure (2) is a rendition of my design of the system. It consists of four main parts: a pipe, piston/rod combination, fly wheel, and motor. The pipe will have two parts. The longest part is to be made out of PVC; this is due to the lightness, inexpensiveness, and ease of machining. The second part is the section that the piston travels in. This part will have to be made out of some type of metal that transfers heat. This is important because heating could change the flow within the pipe and thus change the acoustic properties of the pipe.

The piston/rod combination would have to be made or ordered. Regardless of which is done the metal portion of the pipe will most likely have to be bored-out in order to ensure an exact fit. Even then a small gap must be introduced between the pipe and the piston. This is done so that only the piston rings rub against the walls of the pipe. This must be a highly precise fit, for two reasons. One is that the piston will rub on the pipe which will introduce friction

that could lead to excess heat or binding and then failure. This could be dangerous as the motor would still try to turn and something could break and fly off. The second possibility is that there would not be a good enough seal and air would leak past. This would mean that the piston would not be pushing all of the air and would have less of an effect if any. The piston rod, if purchased, might have to be lengthened. This would be necessary if a longer stroke length was needed than what the piston and rod was designed for. The reason for this is that in order to have simple harmonic motion for a piston, the distance from the center of the crank to the place that the rod meets the fly wheel must be much smaller than the length of the rod. See Figure (3). Lengthening the rod or using a different stroke length than originally designed for can introduce problems that will be discussed later.

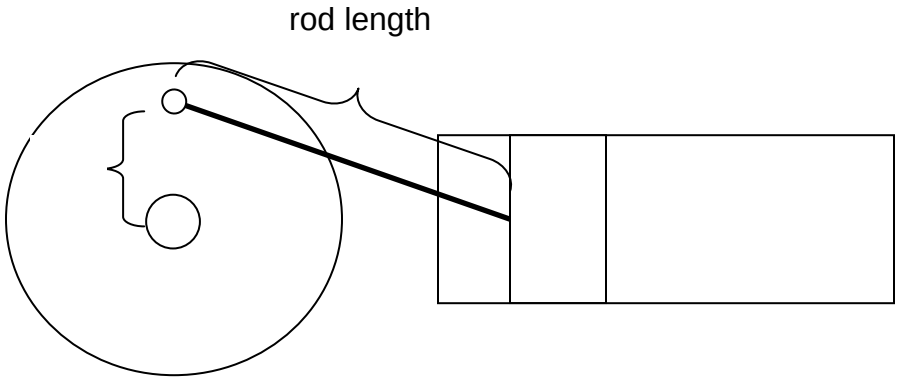

Figure 3. Conceptual drawing used to demonstrate how the ratio between the radius and the rod length affect motion.

The flywheel is a key element of the system. Where it connects to the piston rod determines the length of the stroke. From Figure (4) it can be seen that the stroke length is twice the distance from the center of the crank to where the flywheel and the piston rod connect.

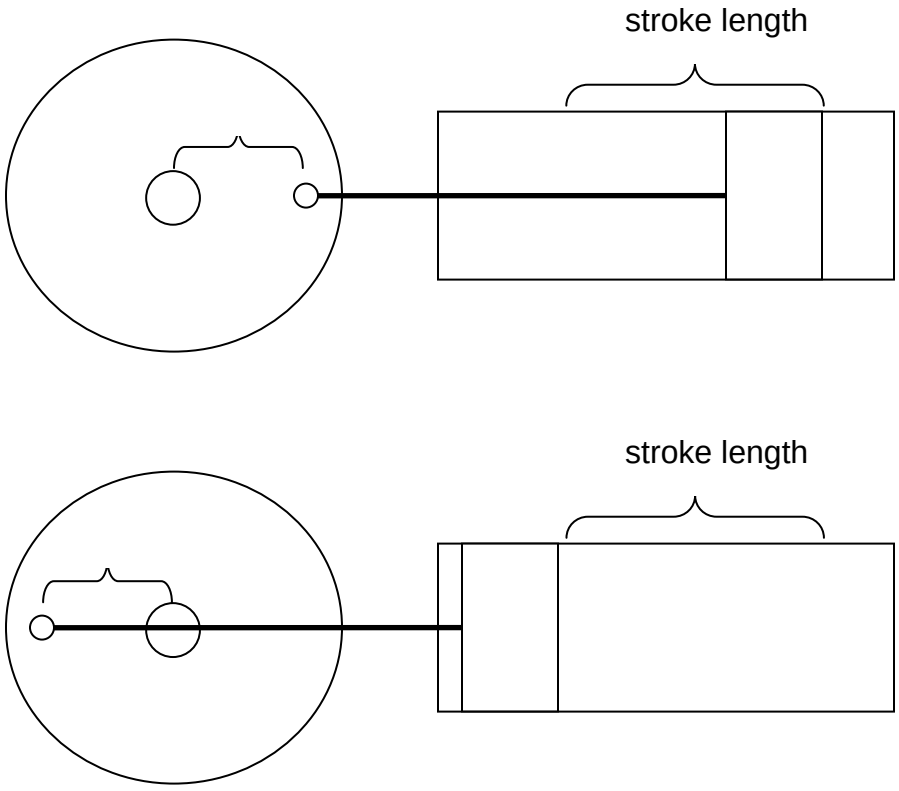

Figure 4. Conceptual drawing used to demonstrate stroke length relative to fly wheel radius.

The other important function performed by the flywheel is to balance the system. Since the piston rod is only on one side of the flywheel the force that it creates is unbalance with respect to the crank. In order to balance this system a weight must be added to the other end of the flywheel. One added benefit to having a system like this is that the stroke length can be made variable. This can be accomplished by either drilling holes in the in the flywheel so that the rod can

be moved from point to point or a slot could be cut out so that the rod could be loosened and slid to a desired point and then tightened in place. See Figure (5).

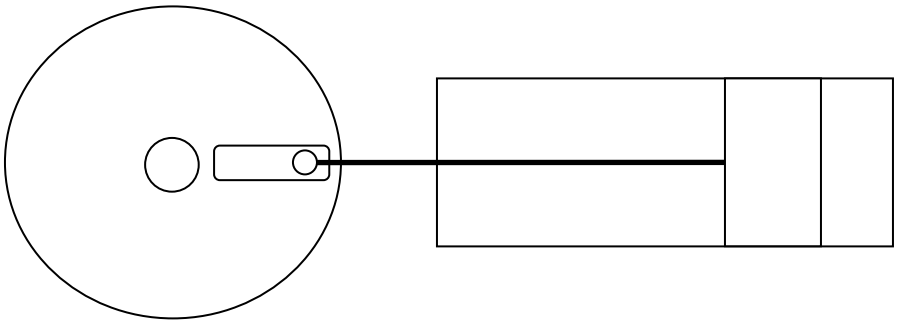

.

Figure 5. Conceptual drawing of slotted fly wheel. The drawing demonstrated how having a slotted fly wheel allows for a variable stroke.

The last component of the system is the motor. This is probably the most open-ended part in the system. This is due to the fact that we must meet all of the other system requirements before we can select the appropriate motor to use. The kind of motor I have in mind for this project is an AC variable speed motor with shaft encoder. The shaft encoder will allow me to know at exactly what RPM the shaft is turning and thus the drive frequency. This is very important because I will be varying the speed in order to find the exact frequency where parametric excitation occurs. The power of the motor is important as well, however, I must know the specifications of the rest of the system before I can make an estimate of the horsepower needed.

A final part of the system that must be considered is how the piston will be lubricated. The standard way in which pistons are lubricated is by oil. In our system this could be problematic. Since the oil will be all over the piston and

cylinder, small particles of the oil will also be in the air which could change the localized acoustic properties of the air. Another method that might be used is to replace the metal piston rings with Teflon piston rings. This would allow for no liquid particles to be introduce to the air, however, at the speed the system will be operating the Teflon will not hold up. So in this particular situation we must accept the small influence the oil might present. Since this is not an off-the-shelf system the oil lubrication system must be designed. The most basic method of achieving this is by developing some type of drip system. The easiest way to do this is by creating an oil pan above the piston travel region and drilling a small connecting hole. The size of the hole will determine the flow rate of the oil. Also note that the size of the hole must be bigger than the width of the piston rings. This is because if there is a difference in pressure between one side of the rings and the other side, and the hole is around the size of the piston ring, then as the ring passes over the hole suction will be introduced. See Figure (6).

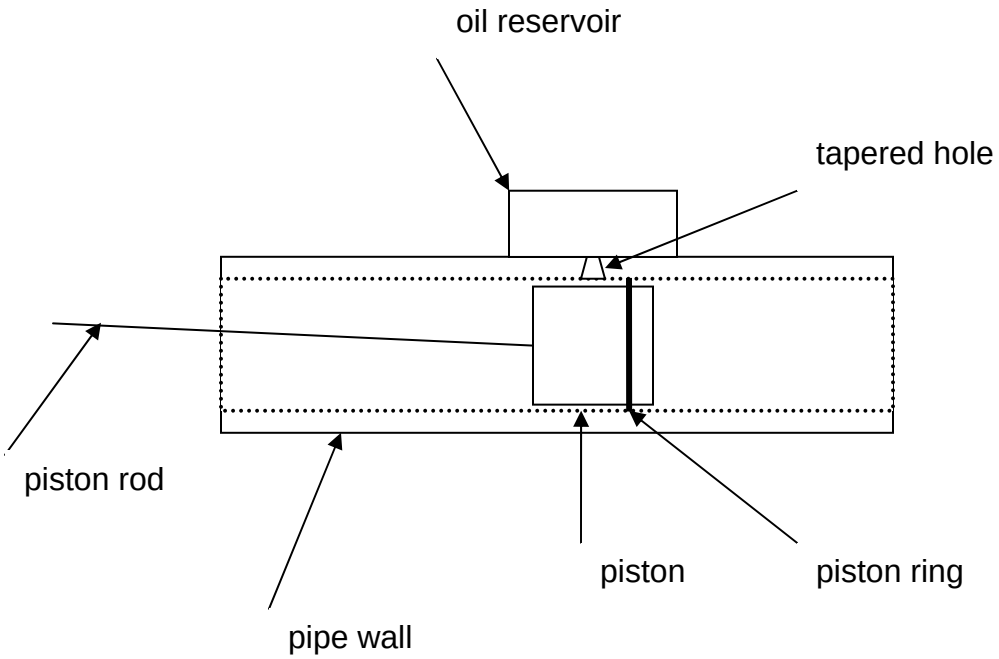

Figure 6. Conceptual drawing of lubrication system. This demonstrates how a oil reservoir and tapered hole can be used to lubricate the system.

Although this system may seem very simplistic, there are several considerations that must be made in order to ensure that it will be safe. One very important consideration is whether it is possible to design a piston and piston rod. This is very complicated and unless it is operating at very low speeds it can cause extreme damage should it break. This is something that would have to be done by a professional with experience in piston design and manufacturing. Another possibility is to purchase a piston and rod that were designed for something else but meet the needed of this project. I have found however, that most pistons do not have a long enough stroke. As mention previously it is possible to extend the length of the piston rod, however, this would have to be done very carefully. If it were misaligned, or the joint not strong enough, or imbalanced, the assembly could fail at high speeds. Another safety precaution that would be needed is some kind of protective box that would have to be built around the piston and motor. This would be to prevent material from flying off if the system did fail.

C. REFINED DESIGN CONCEPT

Due to the problems of the before mentioned system it was decided that a commercial off-the-shelf engine would be used in place of the designed piston assembly. When this portion of the design process was under taken, it was perceived that a 2 inch piston with a 2 inch stroke would be optimal. An investigation of what type of engines had these parameters was begun. To keep this system simple, an additional requirement that the engine be single-piston was added. This was done to reduce the weight of the engine and to decrease the size of motor needed to turn the engine. By doing this, automobile and motorcycle engines were excluded from the possibilities. It was found that hobby engines, used for remote control airplanes and boats were too small. Most only had a maximum diameter of 1.5 inches and a similar size stroke. This reduced the selection of engines to those used for utility purposes. The most common and readily thought of was the standard lawn mower engine. These engines could exceed over 2 inches in piston diameter and stroke length, as well as meet the need for only one piston. For this reason it was decided that a lawn mower

engine would be used for the experiment. See Figure (7) for a rendition of the system. Detailed labeling of each section will follow in other figures.

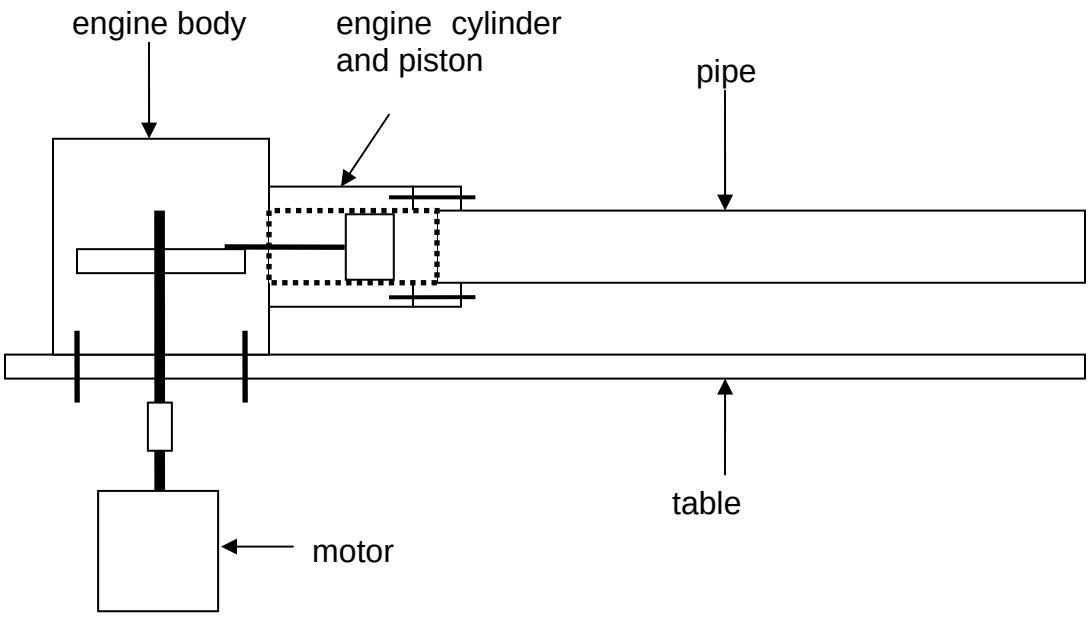

Figure 7. Commercial Off The Shelf (COTS) system. This system is more simple than the initial design concept because only three main components (the engine, motor and pipe) need to be connected.

Although the system may appear to be more complicated than the system from the previous section, it is simpler to construct and operate. Since the engine is preassembled very little needs to be modified in order to use it for the experiment. The following is a description of the function of each component and what modifications if any need to be performed in order to make the system operable.

After having examined several lawn mower engines and selecting the one with the largest piston size and stroke, the process of figuring out how to attach the pipe to the piston cylinder was the next line of action. Upon removing all extraneous parts from the engine (pull cord, head, blade, carburetor and so on),

it was determined that it would be necessary to disable the intake and exhaust valves. This can be accomplished by simply removing the internal gearing that make the valves move. Once this is done a template of the piston head can be made so that an adapter can be machined to connect the piston cylinder and the pipe. Figure (8) shows how the three components connect. The adaptor would most likely be made from plastic so that it can easily be glued to the end of the PVC pipe. The adaptor would then be connected to the head of the piston cylinder using the preexisting bolt holes.

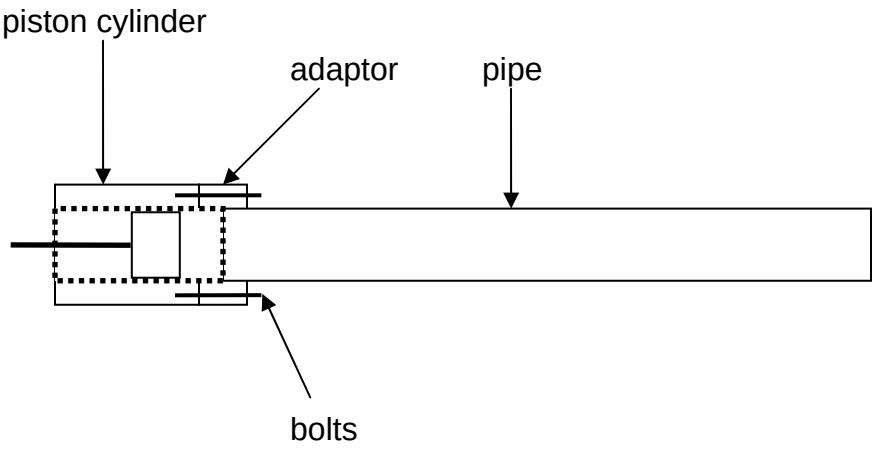

Figure 8. Connection of piston cylinder and pipe.

It is important to note that any jagged edge could cause turbulence in the air. The main location where an edge could disrupt the air flow would be at the junction of the adaptor and pipe, or the adaptor and the piston cylinder. Since the pipe and adaptor are both PVC and will be glued together, they can be bored out at the place they meet so that the transition area is smooth. The place where adaptor and piston cylinder meet is much harder to smooth. The best way to

approach the problem would be to machine the adaptor as precisely as possible. It might also be possible to take the engine apart and to fill any gaps between the piston cylinder and adaptor by hand with filling agent and then sand it smooth by hand. However, this could possible introduce more problems than it would fix. Another consideration is air leaks which could reduce the efficiency of the system. The piston rings ensure that no air will leak pass the piston. The joint between the adaptor and pipe will be sealed with glue, which will prevent any air from escaping. The only other place to consider is the joint between the adaptor and the piston cylinder. Since the joint only exist due to compression from bolts, it is possible that a gap could exist and thus air leakage could occur. To prevent this, a paper or rubber gasket needs to be placed between the adaptor and piston cylinder.

Since the engine is off-the-self and the pipe has already been connected, all that is left to consider is how to attach the engine to the table and connect the motor drive shaft with that of the engine. Figure (9) illustrates how this can be done. Connecting the engine to the table is a fairly simple process. The engine already has mounting holes so once an appropriately sized hole has been drilled into the table the engine can simply be bolted to it. A rubber gasket might be placed between the engine and the table to damp vibration. Before the motor and the engine shafts can be connected, the motor must first be mounted to the table in a secure fashion. Unfortunately until the appropriate motor is selected the means of mounting is unknown. A shaft coupler can be used to connect the motor and engine shafts. These devices are common and can be found easily. The main function of the shaft coupler is to join to shafts together, but allowing them to be slightly misaligned. This is important because two shafts cannot be perfectly aligned. The coupler allows the shafts to wobble while not introducing any lag in the direction of rotation.

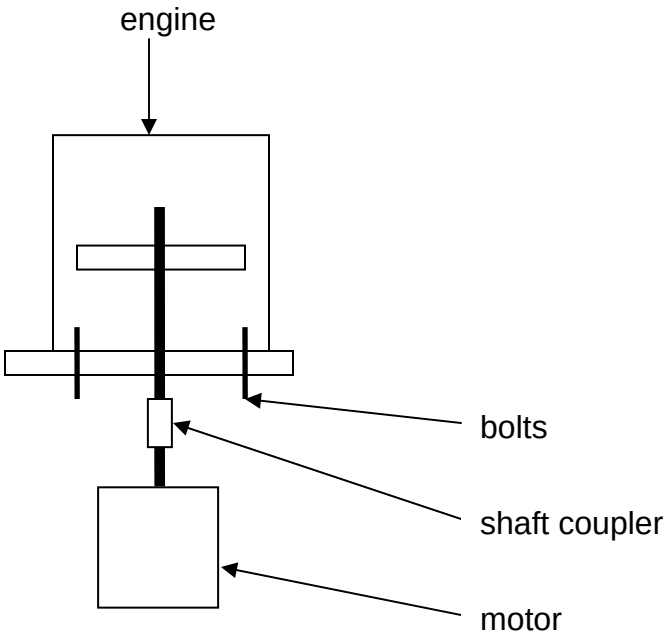

Figure 9. Connection between the motor and engine.

Finally, some comments should be made about motor selection and safety. There are many types and brands of motors. What is important is that the motor be high quality and easy to control. In this particular situation an ac motor is most likely the better choice over a dc motor. The reason for this is size and price. Ac motors tend to be about half the size and cheaper than dc motors. Also, at the operating values of the RPM there is very little difference in performance. Since a fairly large engine will be used, the motor will most likely have to operate on three-phase power. This makes the experiment difficult because that kind of power is not available in most places. For safety reasons the engine and motor will also have to be encased in a protective box. This is absolutely necessary to protect against parts of the system that might fly off should the system fail.

THIS PAGE INTENTIONALLY LEFT BLANK

III. CAPACITANCE-MODULATED CIRCUIT

In this chapter, we consider parametric excitation of an inductor-capacitor (LC) circuit in which the capacitance is modulated.

A. HISTORY AND MOTIVATION

In 1935 a Russian paper was published by L. Mandelstam, N. Papalexi, A. Andronov, S. Chaikin and A. Witt. The title of the paper was "Report on Recent Research on Nonlinear Oscillations". In this paper, the authors discuss many types of nonlinear oscillations. One chapter is dedicated to parametric excitation of nonlinear circuits. I came across references to this paper two different times. Once was when professor Denardo mentioned that one of his books referenced it. The other time was when I was doing a Google search for parametric excitation. The website, http://www.cheniere.org/misc/moscowuniv.htm (29 APR 05) seemed unreliable due to its content, which mostly consisted of claims for free energy without proof. I nevertheless decided to investigate the reference. I found a few more references to the paper on-line but no directions where to find it. After consulting with NPS librarian Michaele Huygen and searching many online resources of the library, I found a copy of the paper in English. The paper had been translated from Russian to French to English. The copy that I had found was produced by NASA Technical Translation.

The paper's discussion of parametric excitation is limited mostly to theory and a general description of the experimental apparatus that the authors constructed. There is also a brief introduction of the history of parametric excitation of electric oscillations. They state, "although the possibility of parametric excitation of electric oscillations has been known for a long time (Rayleigh, Poincare, Brillouin, and later van der Pol), it is only in the last few years that this phenomenon was realized for its full value and its systematic study was undertaken". I proceeded to investigate all of the valid references

from the paper but failed to find any of the papers in English. After thoroughly reading the chapter on parametric excitation I found that the authors had not properly documented the design, construction, or experimentation of the apparatus they had built. This makes it very difficult to reproduce their work to verify their findings. It turns out that several books have referenced this paper but no one has attempted to reproduce the experiment to verify the findings. For this reason it is very important that this experiment is attempted again so that it is well documented for future reference. Another motivation for the construction of a parametrically excited LC circuit is use it as a demonstration in various physics courses.

B. THEORY OF A CAPACITANCE-MODULATED CIRCUIT

To modulate the capacitance of an LC circuit, we consider a bank of n parallel sectored plates, where every other plate is electrically connected, and where one set of plates is rotated (Fig. 10). This configuration amounts to n – 1 identical variable capacitors in parallel (n = 10 in Fig. 10).

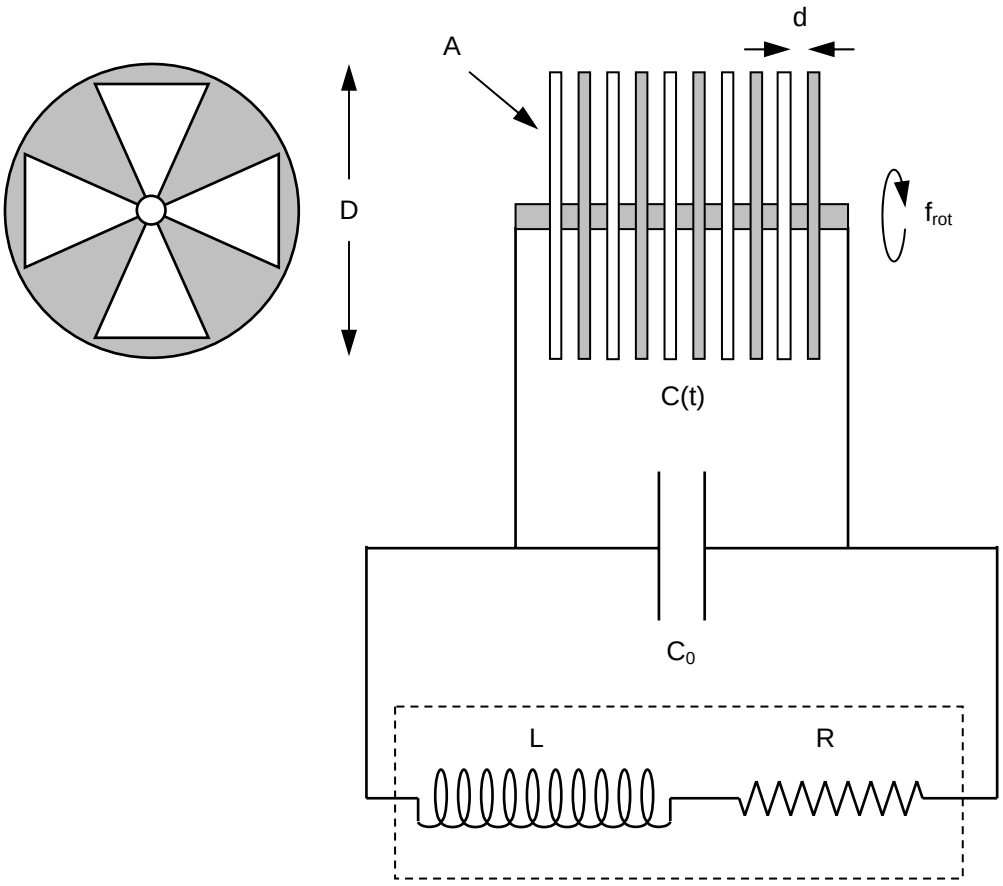

Figure 10. Capacitance-modulated LC circuit. Each plate in the variable capacitor is shown on the left. In the apparatus, every other plate rotates, as shown. The capacitance of the system thus periodically varies from a minimum value of approximately C_0 when the plates do not overlap, to a maximum value of $C_0 + C_{max}$ when the plates completely overlap.

The capacitance of the circuit varies from approximately C_0 for nonoverlapping plates, to $C_0 + C_{max}$ for completely overlapping plates. Because the parallel-plate capacitance is small, we will find that we must choose C_0 to be substantially larger in order to avoid a prohibitively large rotational frequency. Hence, $C_{max} << C_0$, so the average capacitance is $C_0 + C_{max}/2 \approx C_0$, and the natural frequency of the circuit is

$$f_0 = \frac{1}{2\pi\sqrt{LC_0}}. \qquad (3.B.1)$$

Because high rotational frequencies are required, it is important to up-shift the modulation frequency compared to the rotational frequency by arranging the plates to have a number of alternate sectors, as shown in the left diagram in Fig. 10. This effect is utilized in optical choppers. If there are N sectors cut out of each plate with N remaining sectors, where all sectors are approximately the same (N = 4 in Fig. 10), then the capacitance is modulated N times for every rotation, so the relationship between the rotation and modulation frequencies is $f_{rot} = f_{mod}/N$. For optimum parametric excitation, the modulation frequency should be twice the natural frequency (3.B.1) of the circuit. Hence, $f_{rot} = 2f_0/N$ or

$$f_{rot} = \frac{1}{N\pi\sqrt{LC_0}}. \qquad (3.B.2)$$

We now determine the maximum value C_{max} of the variable capacitance. We assume that the plates of the variable capacitor are closely spaced a uniform distance d. The maximum area of overlap of a pair of plates is approximately the area of a sectored plate: $A = \pi D^2/8$, where D is the plate diameter. The maximum capacitance of a neighboring pair of plates is $C_1 = \varepsilon_0 A/d$, and there are n – 1 of these capacitances in parallel. The maximum capacitance amplitude is then $C_{max} = (n - 1)C_1$ or

$$C_{max} = \frac{(n-1)\pi\varepsilon_0 D^2}{8d}. \qquad (3.B.3)$$

The peak parametric drive amplitude is $\Delta C = C_{max}/2$, and the quality factor is $Q = (L/C_0)^{1/2}/R$, where L is the inductance and R is the resistance of the inductor. The standard parametric drive amplitude threshold condition $\Delta C/C_0 > 2/Q$ here is not correct because the modulation of the capacitance is *triangular* rather than sinusoidal in time (Fig. 11). We can correct for this by using the Fourier series

coefficient $8/\pi^2$ of the fundamental frequency of a symmetric triangular wave of unit peak amplitude. The effective amplitude is then $(8/\pi^2)\Delta C$. The parametric drive amplitude threshold condition is thus $\Delta C/C_0 > \pi^2/(4Q)$, which can be expressed as $C_{max} > C_{th}$, where the threshold capacitance amplitude is $C_{th} = \pi^2 C_0/(2Q)$ or

$$C_{th} = \frac{\pi^2 R C_0}{2}\sqrt{\frac{C_0}{L}}. \qquad (3.B.4)$$

Parametric excitation will occur if the modulation frequency f_{mod} is approximately twice the natural frequency (3.B.1), which occurs for the rotational frequency (3.B.2), and if the drive amplitude threshold condition $C_{max} > C_{th}$ is met for the maximum capacitance (3.B.3) and the threshold capacitance amplitude (3.B.4).

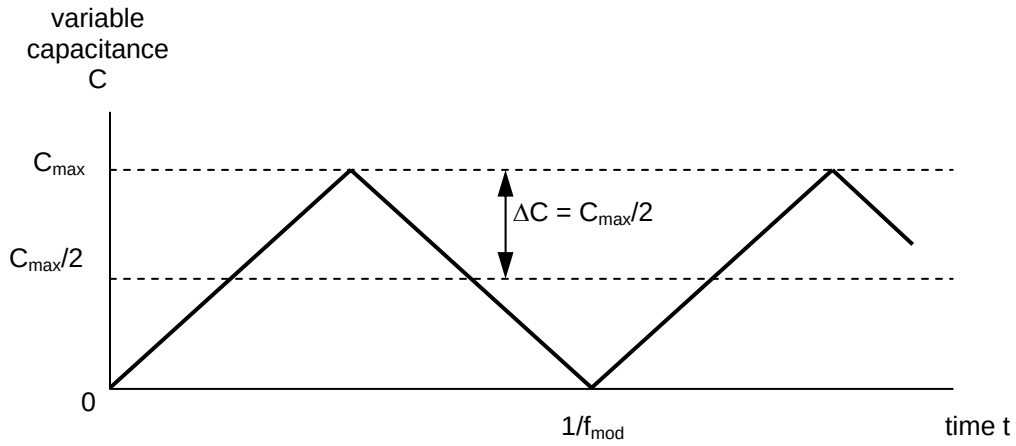

Figure 11. Variation of the modulated capacitance as a function of time. The variation is a symmetrical triangular wave with peak amplitude ΔC.

C. FEASIBILITY OF A CAPACITANCE-MODULATED CIRCUIT

To have a rotational frequency (3.B.2) that is not large, we consider a large value of the inductance: L = 1 H. A large fixed capacitance C_0 also lowers the requisite rotational frequency, but causes a diminished dimensionless drive

amplitude $\Delta C/C_0$. Trial-and-error has lead to the following value: $C_0 = 1\ \mu F = 10^{-6}$ F. The rotational frequency (3.B.2) for N = 10 sectors of removed material is then

$$f_{rot} = \frac{1}{N\pi\sqrt{LC_0}} \approx \frac{1}{10\pi\sqrt{1\times 10^{-6}}} \approx 32\ \text{Hz} \approx 2000\ \text{rpm}\ . \qquad (3.C.1)$$

This frequency is not inordinately difficult to obtain for a rotational apparatus, even for one that is used in a lecture demonstration. Note that the modulation frequency is 10 times the rotational frequency. Because the rotational frequency can be directly measured, the modulation frequency is then conveniently 10 times this value.

We desire to make the capacitance amplitude C_{max} as large as conveniently possible in order to maximize the parametric drive amplitude. Reasonable values of the plate diameter, number of plates, and plate separation distance for a lecture demonstration apparatus are D = 8 in ≈ 0.20 m, n = 100, and d = 0.5 mm = 5 x 10^{-4} m. The maximum capacitance (3.B.3) is then roughly

$$C_{max} = \frac{(n-1)\pi\varepsilon_0 D^2}{8d} \qquad (3.C.2)$$

$$\approx \frac{99\pi\times 8.85\times 10^{-12}\times(0.20)^2}{8\times 5\times 10^{-4}} \approx 2.8\times 10^{-8}\ \text{F} = 28\ \text{nF}\ .$$

To determine the threshold value (3.B.4) of the capacitance amplitude for parametric excitation, we assume an inductor resistance of R ≈ 2 Ω:

$$C_{th} = \frac{\pi^2 RC_0}{2}\sqrt{\frac{C_0}{L}} \qquad (3.C.3)$$

$$= \frac{\pi^2\times 2\times 10^{-6}}{2}\sqrt{\frac{10^{-6}}{1}} \approx 9.9\times 10^{-9} \approx 10\ \text{nF}\ .$$

The maximum capacitance (3.B.6) is a factor of 3 greater than the threshold capacitance amplitude (3.B.7). We conclude that this capacitance-modulated LC circuit is feasible although somewhat difficult to construct as a lecture demonstration.

There are several possible means of increasing C_{max} or decreasing C_{th}, so that the parametric threshold condition $C_{max} > C_{th}$ might be enhanced:

- Cool the inductor with liquid nitrogen, which would lower the resistance R of the inductor, and would thus lower Cth. Although requiring some effort, use of liquid nitrogen in lecture demonstrations is always popular with an audience.
- Decrease the fixed capacitance C0, which would decrease Cth. However, note that a greater rotational frequency would be required. This problem could be alleviated by adding inductors in series in order to increase the inductance and thus lower the frequency. It should be noted, however, that Cth is proportional to L/R1/2, so two inductors in series raises Cth by 21/2.
- Enclose the capacitor in a container filled with a gas of high dielectric constant.
- Have a bank of variable capacitors connected in parallel, which would increase Cmax. Note that the rotations would all have to be ganged so that they are all in phase.
-

D. APPARATUS DESIGN

To better assess the feasibility of building this system a more detailed consideration of the design, manufacturing, assembly, and operation of the system is required. There are three main components to the system: the capacitor, inductor, and motor. Since the inductor and motor will be obtained commercially there is very little to consider about them other than the specification they must meet. The capacitor on the other hand has several issues that must be addressed.

The most basic component of the capacitor are the plates. From a design standpoint it may seem a simple object to create. However, the design of the plates is more complicated then it seems. The plates will be undergoing stresses and strains as they spin. This must be accounted for in the design by using fillets

instead of sharp corners. The width of sectors and how far they are from the axle are of major importance as well. If the narrowest part of a sector is too small then that piece might fail and separate causing damage. If the gaps between the sectors extend too far, making the outer rim small, it could have a similar effect. These factors will be affected by what material the plates are made of. Stronger materials allow the plates to be made thinner, but at the same time they make the plate heavier which affects the size of motor needed.

The manufacturing of the plates must also be considered. Selecting the supplier of the raw material is important. In order to have high quality sheets of the material it is often wise to require mil-spec material when purchasing. The reason it is necessary to have sheets of such high quality is that flaws would create problems later. For example, if the sheet had a slight bow to it when it was being cut the plate would then be bowed as well. A bowed plate, especially with the plate separations used in this system, could rub against the plate adjacent it. At a minimum this would cause a short circuit, at worst it could cause the failure and damage. Other quality issues are density, and uniform thickness, both of which would affect the balance of a plate and thus the balance of the system.

Once a supplier is selected the plates must be cut by a machinist. There available are several methods of cutting plates. These include laser, water jet, chemical milling and milling. Milling is inexpensive but less accurate than the other two. Laser cutting, although highly accurate, can warp the plates due to heat produced during cutting. Chemical milling uses a photolithography and chemical etching technique which does not heat the metal. However, it is a slower or more expensive process. The water jet method has accuracy close to that of a laser but will not warp the plates. For this reason it is the best method for our case.

After manufacturing, the next step is assembly. Some of the difficulties in assembling the parallel plate capacitor are spacing, alignment, and balance. No matter how the plates are attached to the axle, each plate must be placed

individually. This will be a very time consuming process. There are three main ways to attach the plates to the axle. One is to heat the plate, allowing it to thermally expand and thus increase the diameter of the inner hole. Once the hole is sufficiently large the plate can then be slid down the axle to its position. It must then rest there until it has cooled enough to be a tight compression fit. This method is convenient because it does not involve any adhesives. The disadvantages are that the heating must be uniform, the attachment is permanent, and the heat and then moving of the plate can introduce bending. The second method involves using metal conductive adhesive. This has the advantage that it can be undone. The disadvantages are that each plate must dry before the next plate can be placed, adhesives can be difficult to work with, and the plate separation distances used in this system are on the same magnitude as a drop of adhesive which make unwanted connections hard to prevent. The third method of connection is to make the axle have two flat sides and to have a similar shape for the plates inside hole. The plates are then slid onto the axle. The flat sides prevent the plates from spinning relative to the axle. Placing a washer between each plate would guarantee uniform spacing. To keep the plates from sliding along the axle a nut would be placed on the end of the axial at the location of the last plate and tightened. This would create a compression fit. This method is the best choice for this system.

When the plates are being placed on the axle, it is important that they be aligned as closely to perpendicular as possible. The reason for this is demonstrated in Fig. 12. A small misalignment could introduce contact between plates. With the small separation distance that is being using, the plates would rub if they are misaligned by as little as 3 degrees.

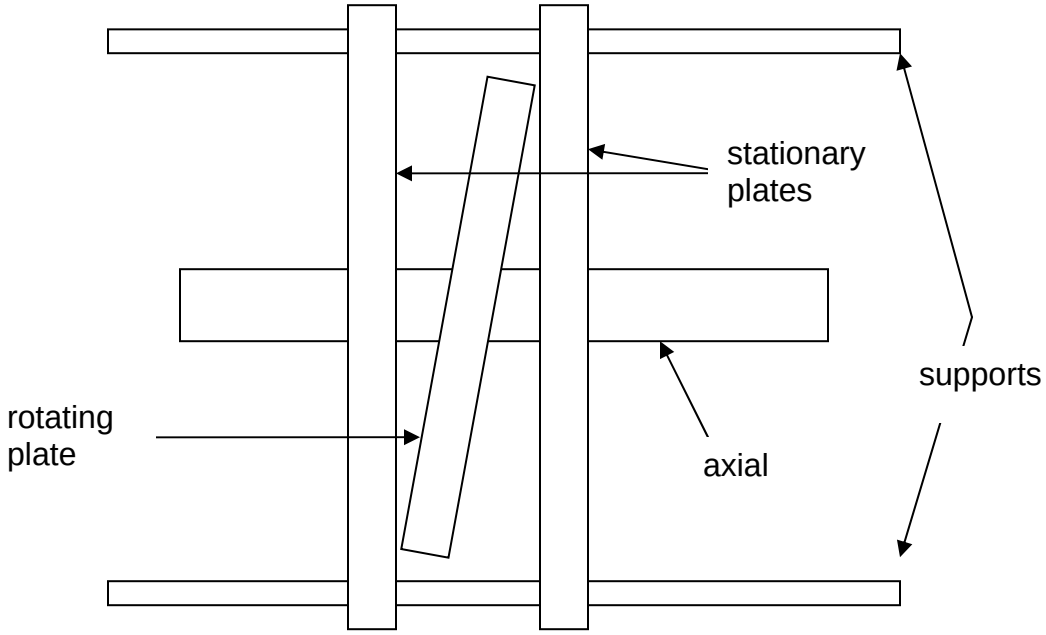

Figure 12. Misalignment of rotating plate leading to contact with stationary plate. View of capacitor as seen perpendicular to axle.

Balance of the capacitor is also important. If the capacitor is not balanced properly then it will wobble. This could lead to mechanical failure. Static balancing would not be sufficient. Dynamic balancing would be necessary due to the speeds the capacitor would be operating at. It is not clear where to ship the assembly to have the balancing done. Imbalance also introduces problems if the capacitor had a plate that was damaged during operation. Since the plate would have to be replaced the capacitor would have to be dynamically balanced again.

Once the parallel plate capacitor is assembled, the next line of action is to mount it to a supporting structure. There are two main methods of supporting the capacitor. One method is to mount it with the axle horizontal to the ground. This method allows the capacitor to be supported by two ball bearings, one on each end of the axial. The bearings are secured to brackets that are secured to the table. This provides for a very strong supporting structure. However, it also leads to a potential problem. Since the weight of the plates is resting on the axle,

bowing of the axle is introduced. This will cause the axle to wobble, possible causing the rotating plates to hit the stationary plates. The way to avoid this problem is by implementing the second method of mounting. This is achieved by mounting the axle vertically. There is a problem associated with this method as well. It is difficult to mount the axle accurately vertically. This could cause the capacitor to naturally lean. The solution to this problem is to build a large support structure around the capacitor. This would reduce the visibility of the capacitor, diminishing its effect as a demonstration. However, it is the better of the two mounting methods.

A final consideration for a cause of mechanical failure is turbulence. As the plates spin past each other the air will be disturbed and the resulting effects on the plates are unknown. The effect could cause the plates to flex and thus cause mechanical failure of the capacitor. Once the capacitor is mounted and the system is connected the next obvious consideration to investigate is operational safety. Due to all of the causes for mechanical failure previously mentioned, it would be prudent to encase the capacitor in a clear polycarbonate safety box similar to the one described for the acoustical apparatus.

Although for this project it not necessary to build or design an inductor, it is important to determine some realistic values of inductance and resistance. For this purpose I gathered a variety of inductors from the physics department. A summery of my findings is listed in table (1). From the table it is obvious that the initial assumption of a 1 H inductor with 2 Ω resistances is unrealistic. Changing the feasibility calculations to reflect this reduces the quality factor and thus increases the required drive amplitude.

Table 1. Resistance of various inductors.

	inductance (at 100 Hz)	ac resistance (at 100 Hz)	dc resistance
Coil inductor	321 mH	118 ohms	6.09 ohms
Powerstat inductor	964 mH	188 ohms	2.18 ohms
Variac inductor	740 mH	195 ohms	1.51 ohms
Toroidial inductor 621	2.84 H	43.0 ohms	17.5 ohms
Toroidial inductor 601	2.95 H	79.4 ohms	18.4 ohms
Toroidial inductor 616	2.61 H	58.9 ohms	18.3 ohms

The final component to consider is the motor. In order to determine what motor to use the power required to rotate the capacitor is needed. In calculating the power it is assumed that the plates are solid, homogenous, and identical. Friction is also neglected. First the mass of an individual plate is found. A density of 2700 kg/m^3 is used for aluminum. The radius and thickness are r = 4 in = 0.1016 m and h = 1/8 in = 0.003175 m, respectively. The mass is thus

$$\rho\pi r^2 h = 2700 \times \pi \times (0.1016)^2 \times 0.003175 = 0.325 \text{ kg} . \qquad (3.D.1)$$

Once the mass is calculated the next step is to find the rotational inertia due to the n = 50 plates that will be rotating. The moment of inertia is

$$I = \frac{n \times \text{mass} \times r^2}{2} = \frac{50 \times 0.325 \times 0.1016^2}{2} = 0.826 \text{ kg} \times \text{m}^2 . \qquad (3.D.2)$$

Next the torque must be calculated. In order to do this constant angular acceleration is assumed. The angular velocity ω is assumed to be the following:

$$\omega = \frac{2 \times \pi \times \text{RPM}}{60} = \frac{2 \times \pi \times 2000}{60} = 209.4 \ \frac{\text{rad}}{\text{s}} . \qquad (3.D.3)$$

It is also assumed that the ramp-up time T is 15 seconds. The torque is thus

$$\tau = \frac{I \times \omega}{T} = \frac{0.826 \times 209.4}{15} = 11.536 \ \frac{kg \times m^2}{s^2} \ . \qquad (3.D.4)$$

Now that we have the torque the power can be calculated:

$$P = \tau \times \omega = 11.536 \times 209.4 \cong 2416 \ W. \qquad (3.D.5)$$

It is wise to convert the power into units of horsepower since most manufacturers specifications are listed that way. The conversion factor is 1 hp = 746 watts, so

$$P = \frac{2416 \text{ watts}}{746 \text{ watts}} \times 1 \text{ hp} = 3.24 \text{ hp} \ . \qquad (3.D.6)$$

This motor is within a reasonable size however, if the required size motor increased by 1/2 hp then three phase power would most likely be required.

Taking into consideration all of the potential problems it has been decided that it is too large of an engineering undertake for the potential gain. We thus moved to the third and final parametrically excited system.

THIS PAGE INTENTIONALLY LEFT BLANK

IV. TORSIONAL OSCILLATOR

In this chapter, we investigate parametric excitation of a torsional oscillator in which the length of the oscillator is modulated. The concept and motivation for this work are stated in Sec. A, the theory is developed in Sec. B, the construction of the apparatus is detailed in Sec. C, and demonstrations and experiments are discussed in Sec. D.

A. CONCEPT AND MOTIVATION

A torsional oscillator consists of a length of flexible material with one end fixed and the other attached to a body, where the system performs angular oscillations about the central axis. The frequency depends upon the length of the material; specifically, the frequency increases for shorter lengths and decreases for longer lengths. Hence, by modulating the length at twice the natural frequency of the oscillations, we should be able to parametrically excite torsional oscillations if the modulation length is sufficiently large.

A preliminary sketch of how such a system could be constructed is shown in Fig. 13. The torsional oscillator consists of a vertical strip of material with a dumbbell attached to the lower end. The location of the upper end of the active segment of the strip is vertically oscillated by a double-roller assembly driven by a dc motor. It is interesting to consider the case where the material is not a strip but is a cord or wire of circular cross section. It is doubtful that parametric excitation can be achieved in this case, but an experiment to resolve this issue is left for future work.

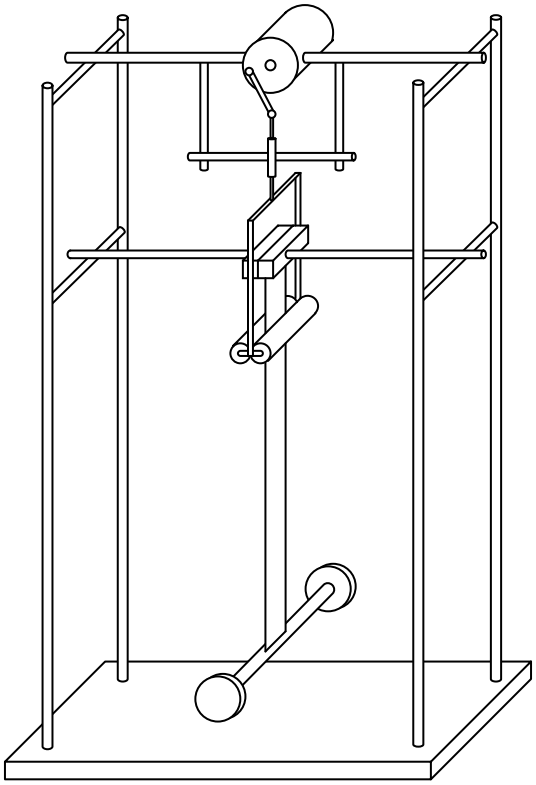

Figure 13. Length-modulated torsional oscillator. The motor (top) and linkage cause the double-roller to vertically oscillate, and to thereby modulate the length and thus the frequency of the torsional oscillator.

One of our motivations is to construct a lecture demonstration apparatus. An important advantage of such an apparatus is that it typically has low frequency (on the order of 1 Hz), which allows a high-amplitude drive to be readily built. In addition, the damping is typically not high. We are thus almost assured that the threshold for parametric excitation can be easily exceeded, in contrast to our other attempts of a parametrically excited acoustic resonator (Ch. II) and inductor-capacitor circuit (Ch. III). Another motivation is to compare the experimental data to theoretical predictions. The theory is based on weak linear damping, weak nonlinearity, and a drive frequency near twice the natural frequency. It may be that an actual system substantially deviates from this regime.

B. THEORY

We consider a torsional oscillator with linear torsional constant κ (torque per unit angular displacement) and moment of inertia I of the attached body about the axis of rotation. If θ is the angular displacement from equilibrium, Newton's second law for rotational motion (torque equals moment of inertia multiplied by angular acceleration) yields the equation of simple harmonic motion for small-amplitude oscillations:

$$\ddot{\theta} + \omega_0^2\theta = 0, \tag{4.B.1}$$

where the natural angular frequency is $\omega_0 = (\kappa/I)^{1/2}$. The linear torsional constant is inversely proportional to the length of the material that undergoes twisting, just as the spring constant of a spring is inversely proportional to the length of the spring. The torsional constant is thus $\kappa = \alpha/L(t)$, where L(t) is the length and α is a constant that in general depends upon the material and the cross-sectional geometry. If the length varies as $L(t) = L_0 - \Delta L\cos(\omega t)$, where $\Delta L << L_0$, the equation of motion (4.B.1) approximately becomes Mathieu's equation

$$\ddot{\theta} + \omega_0^2\left[1 + \eta\cos\left(\omega t\right)\right]\theta = 0, \tag{4.B.2}$$

where the ambient natural frequency is

$$\omega_0 = \sqrt{\frac{\alpha}{IL_0}} = \sqrt{\frac{\kappa_0}{I}}\ . \tag{4.B.3}$$

In Eq. (4.B.2), the ambient linear torsional constant is $\kappa_0 = \alpha/L_0$, and the dimensionless parametric drive amplitude is

$$\eta = \frac{\Delta L}{L_0} . \qquad (4.B.4)$$

To better quantify the system, we should include damping and nonlinearity. The damping dictates the threshold value of the dimensionless parametric drive amplitude (4.B.4) for which parametric excitation from rest will occur. The nonlinearity dictates the steady-state response amplitude, in which the damping also plays a role. (As discussed in Ch. I, only a nonlinearity can limit the growth in parametric excitation.)

In contrast to acoustic parametric excitation of an acoustic resonator (Ch. II) and an inductor-capacitor circuit (Ch. III), the damping in a typical demonstration-sized torsional oscillator is expected to be approximately *quadratic* in the velocity rather than linear. Linear damping may only occur for very small amplitudes. The standard theory of parametric excitation may thus not apply. Although a theory may be achievable for this type of nonlinear damping, it would not be straightforward.

In addition to the nonlinear damping, there is another theoretical complication. The restoring torque for a suspended torsional oscillator as in Fig. 13 arises from *two* different sources: the shear modulus of the material, and gravity. The gravitational restoring torque is purely geometrical, and is due to fact that the body rises in the gravitational field as the material is twisted. The gravitational potential energy thus increases, which implies a restoring torque. Although the shear torque for small amplitudes can be calculated, it is difficult to determine the torque for finite amplitudes; specifically, the nonlinear coefficient of the cube of the angular displacement. (There is no quadratic nonlinearity due to symmetry.) However, because the gravitational torque is purely geometrical, this nonlinear coefficient can be readily calculated, as we now show.

The geometry is shown in Fig. 14. A body (not shown) of mass m is attached to the bottom segment of the strip. Because the body rises due to the twisting of the strip, the increase in gravitational potential energy is

$$U = mgh\,, \tag{4.B.5}$$

where h is the height that the body rises, which is the same height that the bottom segment of the strip rises. We require to determine h in terms of the angle θ for small but finite angular displacements, because the gravitational restoring torque is

$$N(\theta) = -\frac{dU}{d\theta}\,, \tag{4.B.6}$$

from which we can then determine the linear restoring torque and cubic-nonlinear correction to this torque.

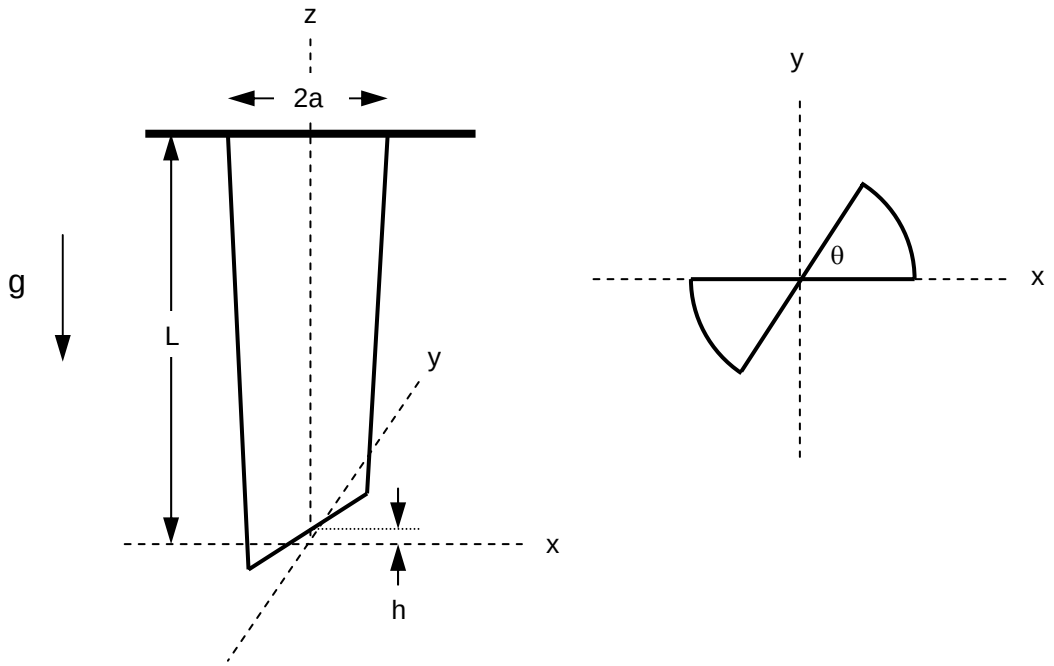

Figure 14. Uniform twisting of a strip of material in a torsional oscillator. On the left is a front perspective view. The bottom segment of the strip, where the body (not shown) is attached, rises a height h due to the twisting. On the right is the top view. The bottom segment rotates an angle θ.

In Fig. 14, to determine the height h of the bottom segment of strip as a function of the angular displacement θ, we note that the length of a long edge of

the strip has a constant value L_0. The distance between the anchored point (x, y, z) = (a, 0, L_0) of an edge and the lower point (a cos(θ), a sin(θ), z) must therefore also be L_0, so

$$L_0^2 = \left[a - a\cos(\theta)\right]^2 + a^2\sin^2(\theta) + \left(L_0 - h\right)^2 . \qquad (4.B.7)$$

This expression holds for $-\pi \le \theta \le \pi$; for greater angular displacements, the strip touches itself, which invalidates the expression. Performing the square in Eq. (4.B.7), simplifying, using the identity $1 - \cos(\theta) = 2\sin^2(\theta/2)$, and solving for h yields

$$h(\theta) = L_0\left[1 - \sqrt{1 - \frac{4a^2}{L_0^2}\sin^2\left(\frac{\theta}{2}\right)}\right]m . \qquad (4.B.8)$$

The power-series expansion of Eq. (4.B.8) in θ to fourth order must be done with care so that all of the contributions are included. The expansion is

$$h(\theta) = \frac{a^2}{2L_0}\left[\theta^2 - \left(\frac{1}{3} - \frac{a^2}{4L_0^2}\right)\theta^4\right] . \qquad (4.B.9)$$

The torque is given by Eq. (4.B.6), where the potential energy is given by Eq. (4.B.5). Substitution of Eq. (4.B.9) yields

$$N(\theta) = -\frac{mga^2}{L_0}\left[\theta - \left(\frac{4}{3} - \frac{a^2}{L_0^2}\right)\theta^3\right] . \qquad (4.B.10)$$

This expression gives the restoring torque in a torsional oscillator with a perfectly flexible strip, to fourth order in the angular displacement. We see that the linear torsional constant is

$$\kappa = \frac{mga^2}{L_0}, \qquad (4.B.11)$$

$\kappa = mga^2/L_0$. The experimental value of the linear torsional constant of any strip being tested in the apparatus can be determined from the linear frequency (4.B.3) by computing the moment of inertia and then timing a number of cycles of small-amplitude motion, where the linear period is $T_0 = 2\pi/\omega_0$. This value of the torsional constant can then be compared to the theoretical value (4.B.11) for zero shear modulus. This method offers a way of comparing the relative importance of the shear and gravitational torques.

The nonlinear coefficient in Eq. (4.B.10) reveals that the system *softens* if $L_0 > (3/4)^{1/2}a$, which holds in the typical case $L_0 >> a$. The nonlinear coefficient allows the steady-state amplitude to be predicted if the damping were linear.

C. CONSTRUCTION OF THE APPARATUS

An overall picture of the system is shown in Fig. 15. The construction of the apparatus was implemented in three phases. Phase one consisted of constructing the support structure, which is the foundation for the system. There are two key features of the support. One is the leveling system. A two-dimensional level was installed so that the user could determine if the apparatus was level or not. If it was not level then the user could adjust one of three bolts on the bottom, two in front and one in back. This provides for an easy method of leveling. The second feature is the acrylic supports for the motor, and rollers. The two pieces of acrylic both provide support and allow a clear view of the system while it is functioning. The support system laid the foundation for the next phase, which was the roller guide and ribbon clamp.

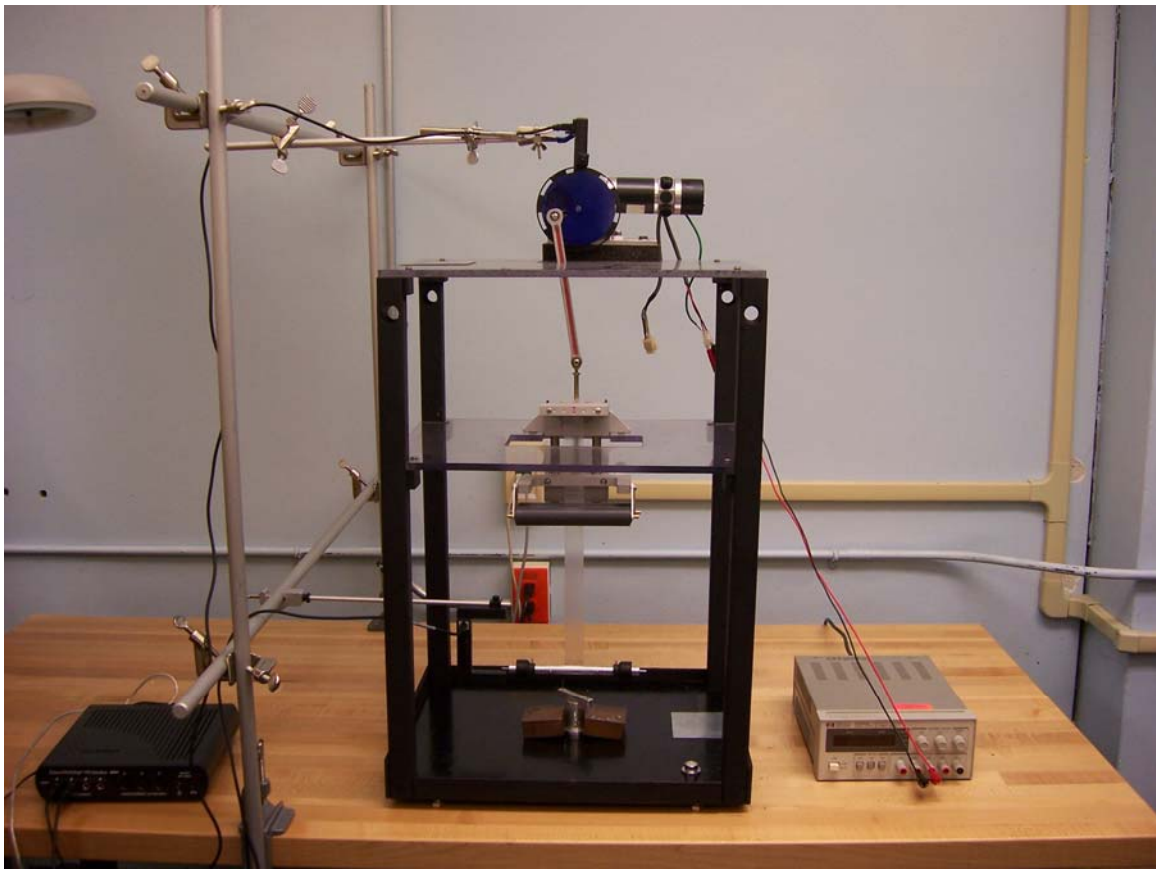

Figure 15. Length-modulated torsional oscillator apparatus.

The rollers are made of PVC with ball bearings in the ends to provide for smooth rolling over the ribbon (Fig. 16). The rollers were machined exactly the same so that there would be no nonuniformities. The rollers are hung by hinges from a traveling “U” shaped support. The support travels along two cylindrical guides that are attached to the ribbon clamp which in turn is attached to the overall support structure. The “U” shaped support is driven by a single cylindrical rod that is in turn driven by the drive system.

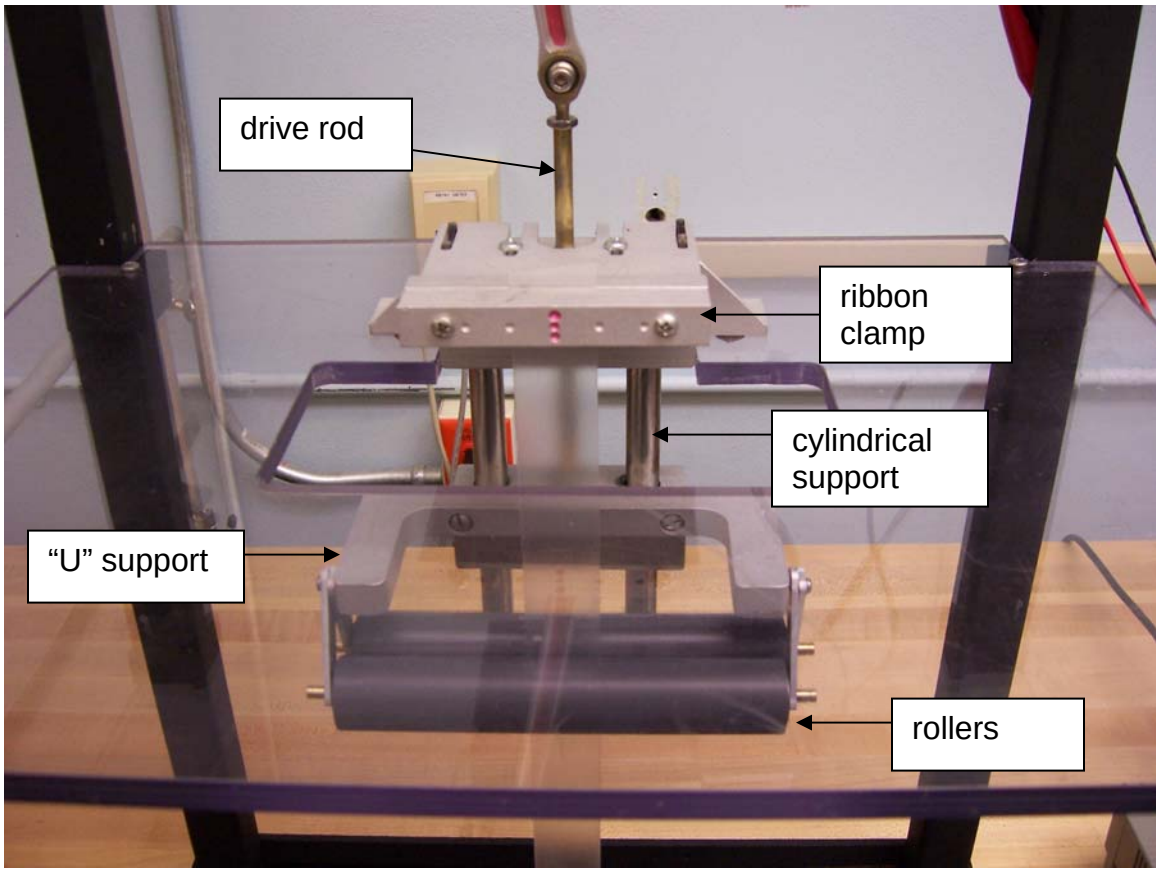

Figure 16. Frontal view of “U” support and ribbon clamp.

The final phase of construction involved creating the drive system. Due to the importance of finishing the construction in time to collect data, and the reduced amount of time left, it was decided to use what was available for construction instead of performing an analysis to determine the best suited equipment. A motor that had been previously attached to a robotic arm was used for the driving motor. This was thought to be a wise decision because the motor has a high-accuracy encoder built on it, so it could be used later to determine very accurate data. Since the motor that was chosen was low torque it was decided to use a high gear ratio gear box to increase the torque and slow the motor down. The gear ratio is 60:1. The motor is not directly coupled to the gear box. It is mounted instead at a ninety degree angle so that the apparatus would have a cleaner look and so that all the working parts would be easily

visible. The drive wheel is attached to the opposite side of the gear box. It has a slot cut out of it for the purpose of attaching the drive armature. Grooves were cut into the drive wheel and drive armature so that when the drive armature is in its most vertical position the grooves would line up, which allows the distance from the center of the bearing to the center of the drive wheel be determined. This allows the user to set the modulation length. See Fig. 17 and Fig. 18 for pictures of the components.

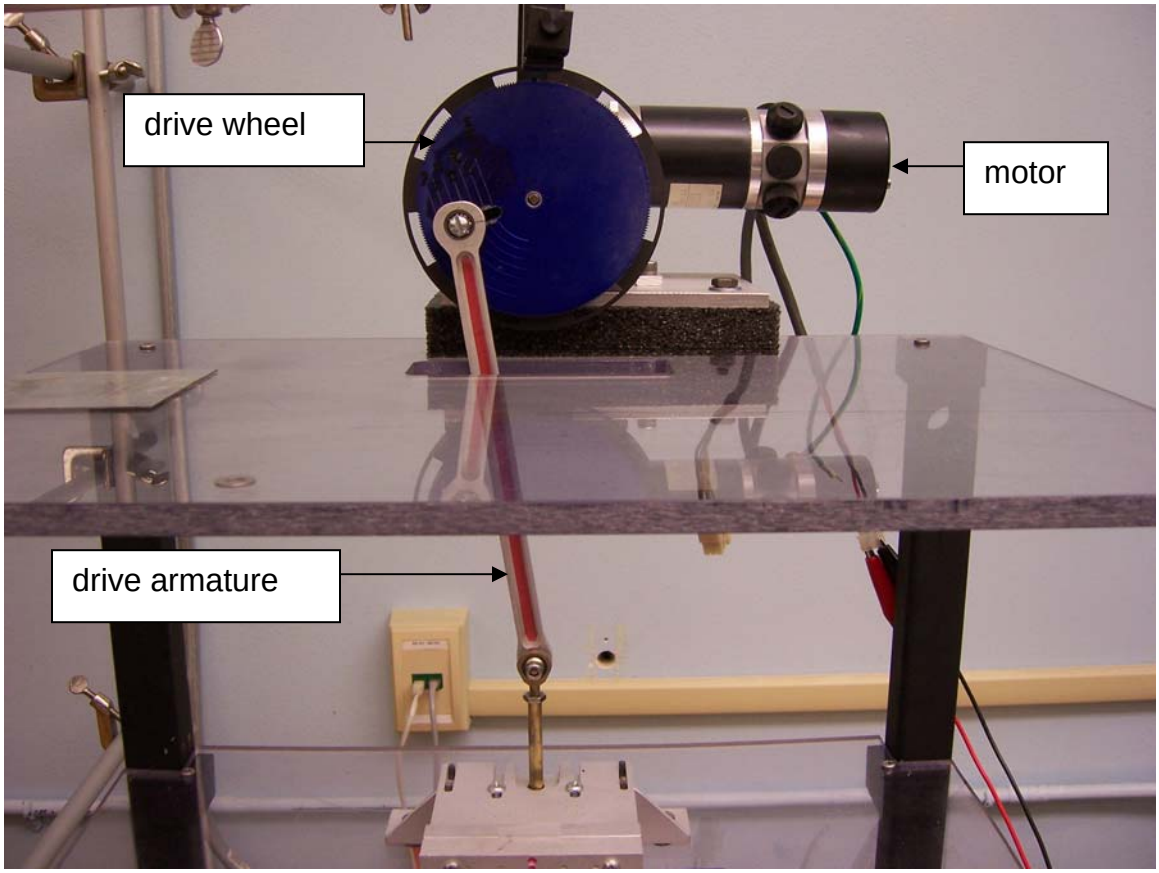

Figure 17. Frontal view of drive system.

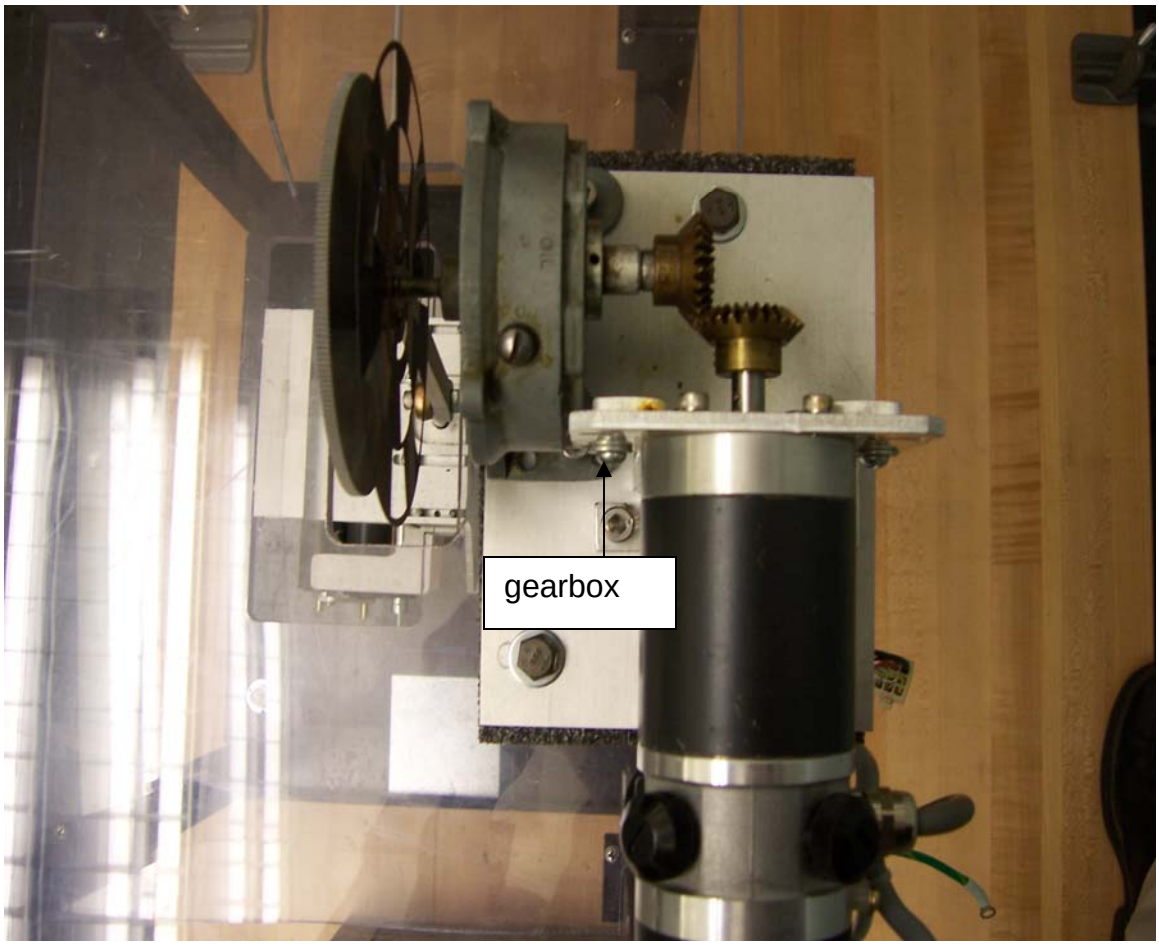

Figure 18. Top view of drive system.

A few added design features must be mentioned about the system. First is the adjustable positioning of the masses on the dumbbell (Fig. 19). This allows the user to change the natural frequency of the system with out having to change ribbon length or material. The user can do this by removing the pin that goes through the mass, slide the mass to the next hole and replace the pin. The next feature that was added is a controlled release mechanism (Fig. 19), which allows the user to release the pendulum from a specific displacement in a controlled and repeatable fashion. This is done by placing the device in the desired release position, raising the inner cylinder, and then placing a pin through the outer cylinder into the inner cylinder to hold it in place. Once it is positioned exactly where the user wants it, the pin is then removed, which drops the inner cylinder

and releases the pendulum. The final addition to the system is the photogates and data collection system, which will be described in more detail in Sec. D. See Fig. 19 for images of added design features.

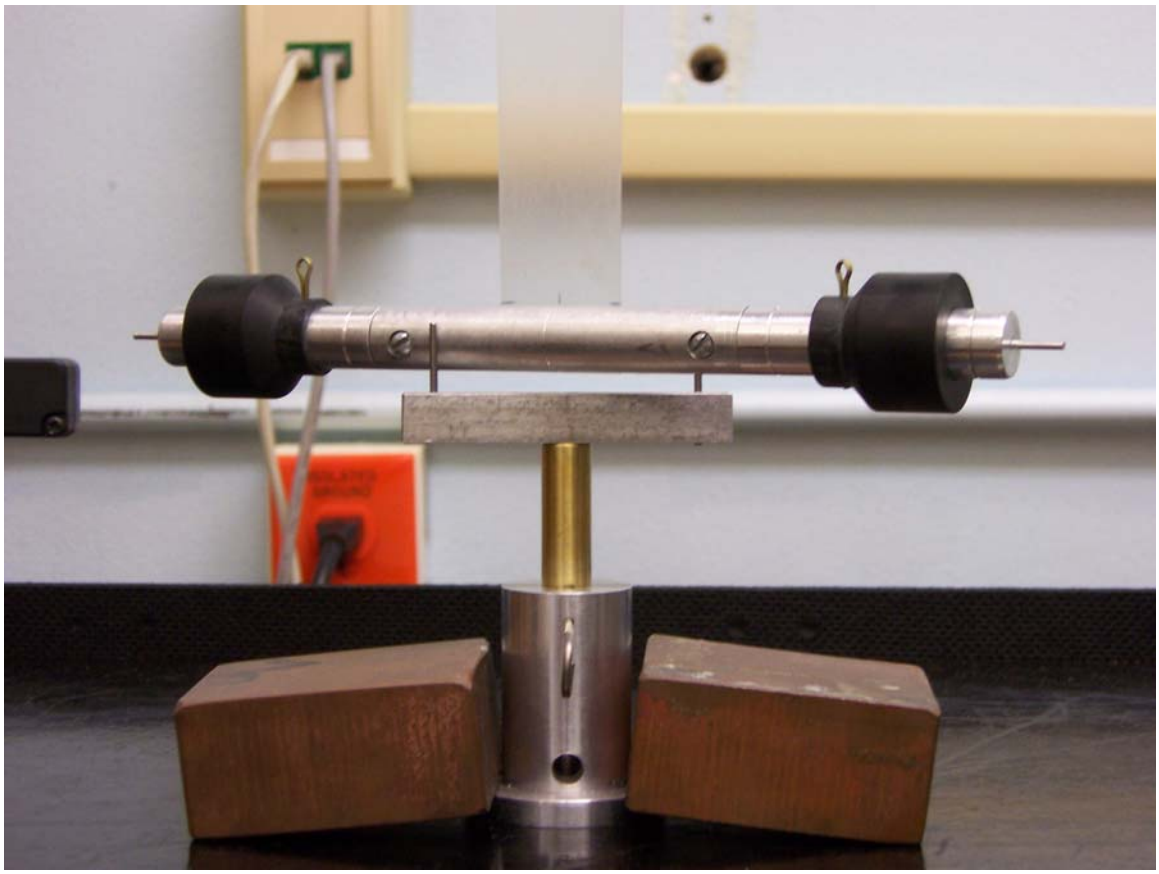

Figure 19. Movable masses and controlled release device.

D. DEMONSTRATIONS AND EXPERIMENTS

The data for the experiment is collected using photogates and a data collection interface that interprets the signal from the photogates into usable information. This information is then sent to the computer where the user can plot it. The data gathered by the photogates is interrupt time information. This is used by the computer software to determine the velocity and period information. The velocity that is important in this experiment is the peak instantaneous velocity. However, the information gathered by the photogate is average velocity. This is because the software takes the diameter of the pin at the end of

the dumbbell and divides it by the time it takes to pass the detector. Since the pin has a finite diameter the velocity calculated is actually an average velocity. However, because the diameter of the pin is small (1/16”) the average velocity and instantaneous velocity will differ only slightly, so for calculation purposes the average velocity will be treated as an instantaneous velocity. The period for the dumbbell is calculated by the time between two interrupts. Due to the way that the photogate triggers and the timers are activated only one-half of an oscillation can be measured for period information, so the measured time must be doubled. The period of the drive system is calculated in the same way as an encoder would. Period data is then translated into frequency data by the computer software.

In order to describe this system there are a few necessary parameters that need to be determined experimentally. The first is the natural frequency of the torsional oscillator ω_o. This can be determined from the free-decay of the velocity as a function of frequency. As velocity goes to zero the frequency of the oscillator goes to the natural frequency, see Fig. 20. From this information it was determined that the natural frequency is $\omega_o = 0.132$ Hz.

As important fact from Fig. (20) is that the system *hardens*; that is, the natural frequency increases for greater amplitudes. The theory of a perfectly flexible strip (Sec. B) yields softening due to gravitation. We thus conclude that the shear modulus of the material dominates the gravitational effects

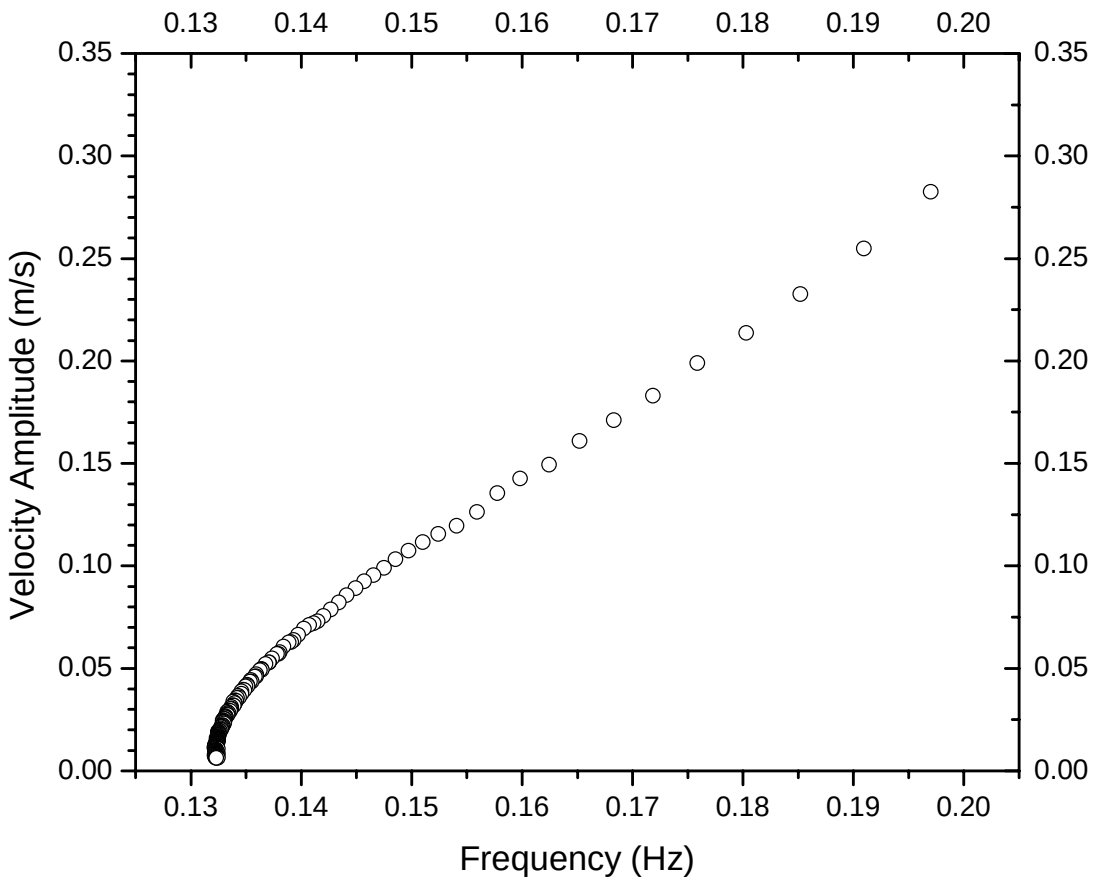

Figure 20. Free-decay data. The natural linear frequency of oscillator is determined from the zero velocity intercept.

The next parameter that needs to be determined is the linear damping coefficient β. This can be determined from a free-decay plot of the velocity verses time. When the system is oscillating at low amplitude the decay of the velocity verses time should be linear on a semi-log plot. The slope of this line is the linear damping coefficient β. From the data β is determined to be 4.1×10^{-3} s^{-1}. See Fig. 21.

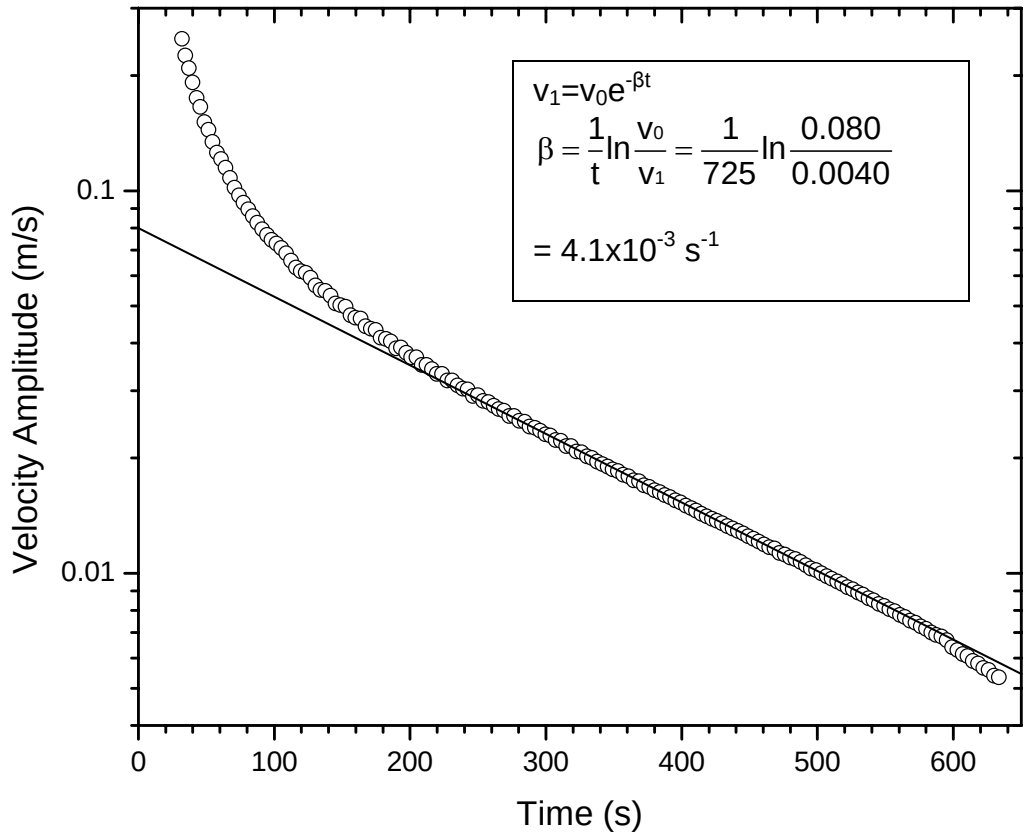

Figure 21. Free-decay plot of velocity verses time. The damping parameter β is calculated from slope.

The last parameter that needs to be determined is the nonlinear coefficient α. This is calculated from the slope of the small-amplitude region of the velocity amplitude squared verse frequency plot, see Fig. 22. The displacement amplitude is approximately

$$A = \frac{v_0}{2\pi f_0}. \qquad (4.D.1)$$

Substituting this into equation (1.A.8), the velocity amplitude squared as a function of frequency can be determined. This equation then takes the form of a linear equation with

$$\text{slope} = \frac{-128\pi^4 f_0^3}{3\alpha}. \qquad (4.D.2)$$

From this α is determined to be -17.38 Hz^4s^2/m^2.

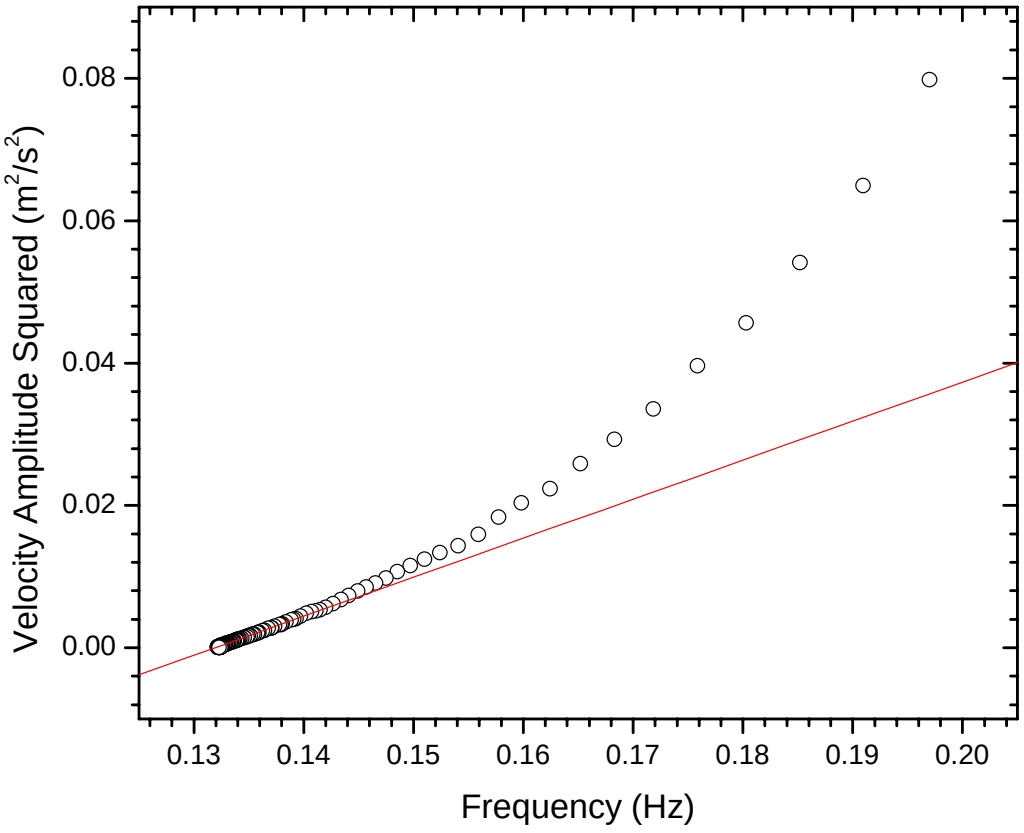

Figure 22. Velocity amplitude squared verses frequency. The slope is used to calculate the nonlinear coefficient α.

Now that those three parameters have been determined the system can be described by its steady state response and excitation response. The plots associated with these are tuning curves and the drive plane of dimensionless parametric drive amplitude η verses drive frequency f. See Fig. 23 and Fig. 24. The equations used to create the theoretical curves are equations (1.A.9) and

(1.A.4), respectively, where the appropriate substitutions were made so that they would be in terms of frequency and velocity amplitude. In the tuning curve graph the triangles indicate data taken for decreasing frequency after the response has fallen off the tuning curve.

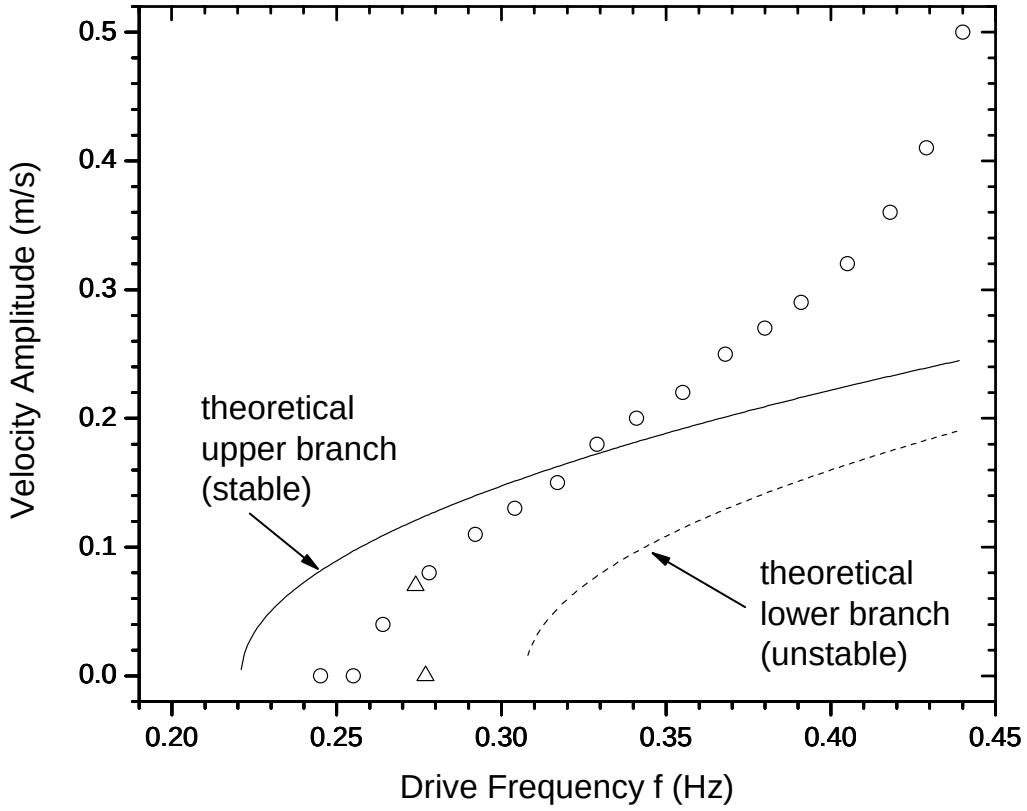

Figure 23. Steady-state response. The curves are theoretical and the points are experimental. The dimensionless parametric drive amplitude η =0.146 .

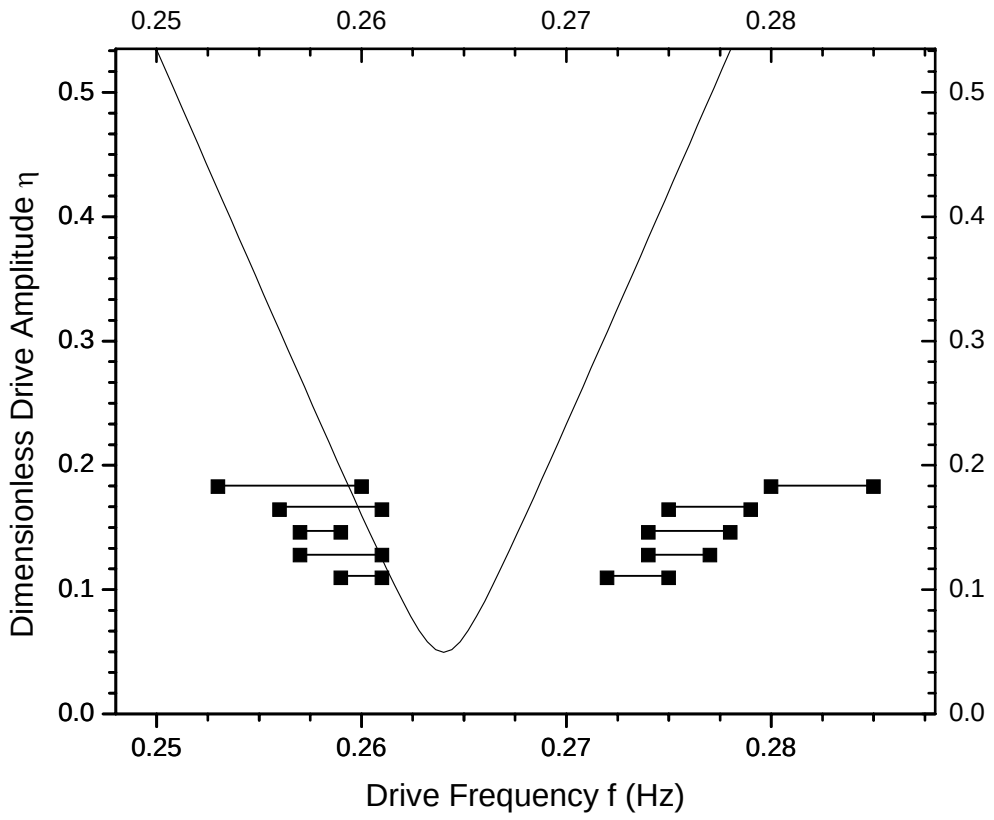

Figure 24. Drive plane plot of η verses f. The curve is theoretical, and the points are experimental.

From the graphs it is clear that the system is behaving differently than the theory predicts. This could be due to strong nonlinearities or possibly it is related to the level of accuracy that the data was taken at. Since the experiment was put together expeditiously, high precision equipment was not available. In Chapter V I will discuss recommendations for any continued efforts with this experiment.

What can be learned from the data is exactly how the system behaves and thus what to expect when operating it. This is essential for demonstration purposes. This apparatus can be used to demonstrate, in a controlled, reproducible method, excitation from rest. It can also demonstrate the characteristics of the tuning curve. By this it is meant that it can be shown to increase in response velocity amplitude as frequency is increase to the point

where the system becomes detuned and thus velocity amplitude drops to zero. The hysteresis effect can then be demonstrated by lowering the drive frequency to the point where the system starts responding again.

The steady-state amplitude graph in Fig. 23 and the threshold data in Fig. 24 both show substantial deviations between the experimental data and the theory. However, it should be noted that there are many approximations in the theory: (i) The theory assumes weak linear dissipation, whereas the apparatus exhibits strong nonlinear dissipation at larger amplitudes, as shown in Fig. 21. (ii) The theory assumes a weak cubic nonlinearity, whereas a very strong deviation from this is evident in Fig. 20. (iii) The theory assumes a weak drive amplitude ($\eta << 1$). The typical values of η for the apparatus are 0.1. (iv) The theory assumes that the drive frequency is near twice the natural linear frequency. In the experiment, the average deviation of the drive frequency from twice the linear natural frequency is roughly 4%. Of all the deviations, it appears that only the final approximation (iv) is met by the apparatus. Approximation (iii) may be roughly met. Due to the other deviations, however, we should not expect good agreement of the steady-state amplitudes in Fig. 23. The threshold data in Fig. 25 should *not* depend upon nonlinearity, either in regard to the cubic nonlinearity or the nonlinear damping. An understanding of the discrepancies is challenging, and more data are required. This is a subject of future work.

THIS PAGE INTENTIONALLY LEFT BLANK

V. CONCLUSIONS AND FUTURE WORK

A. CONCLUSIONS

One inherent difficultly of parametric excitation is that, without a detailed examination of a system, it is not obvious how difficult it would be to excite the system. That is why research of this nature is important. Without investigating different types of systems, it is unclear what might be possible. From these investigations we have learned that it will require either a significant engineering undertaking or a discovery of a new parameter to vary in order to excite acoustical standing waves in a resonator. We have also learned that parametric excitation of an LC circuit by capacitance modulation would also require a significant engineering undertaking. However, due to our calculations and the claims previously made, it seems that it might be possible. Finally, in regard to a length-modulated torsional oscillator, we have demonstrated that it is possible to design and build a controlled, quantifiable, and reproducible demonstration apparatus for the explicit purpose of educating students on the topic of parametric excitation.

B. FUTURE WORK

Several projects can be undertaken as future work. Although several attempts at parametric excitation of acoustic standing waves have failed, I am of the firm belief that it is possible. However, the concept of modulating the length of a resonance tube has been exhausted, unless a serious engineering challenge is accepted. In order for excitation to readily occur a new parameter or method of modulation must be uncovered.

The LC circuit has potential but it is probably worth investigating inductance modulation before pursuing capacitance modulation any further. I say this because of how large of an undertaking it would be to construct the parallel plate capacitor and because in the paper referenced in Ch. III the author had higher levels of excitation in the inductance-modulated circuit.

Finally, more data needs to be taken on the length-modulated torsional oscillator so that a more accurate description is available to compare to the theory. Future experiments might include using different ribbon material and lengths of ribbon and drive amplitudes. Also, as mentioned in Ch. IV, an experiment should be done on materials of cylindrical shape such as wire, or cord. Some system modifications that need to be made are: (i) Obtain a better motor. The one currently in use is underpowered. (ii) Attach an encoder to the shaft with a readout of some kind, that way the audience can see the frequency at which the system is operating. (iii) The apparatus could be made smaller so that it is more portable.

LIST OF REFERENCES

Denardo, B., and Larraza, A., *Nonlinear Oscillations and Waves: An Essential Introduction with Demonstrations* (Naval Postgraduate School, Department of Physics, 2004). This text is used for the NPS course PH4459 (Nonlinear Oscillations and Waves).

http://www.cheniere.org/misc/moscowuniv.htm (last accessed 29 APR 05)

Mandelstam L., Papalexi N., Andronov A., Chaikin S., and Witt A., "Report on Recent Research on Nonlinear Oscillations" NASA Technical Translation, NASA TT F-12, 678. November 1969.

Smith, D., "Parametric Excitation of an Acoustic Standing Wave," M.S. thesis, Department of Physics, Naval Postgraduate School, June 2003.

Varnadore, P., "Feasibility Investigations of Parametric Excitation of Acoustic Resonators," M.S. thesis, Department of Physics, Naval Postgraduate School, June 2001.

Wright, W. B. and Swift, G. W., "Parametrically driven variable-reluctance generator," *J. Acoust. Soc. Am.*, vol. 88, no. 2, pp. 609-615 (1990).

THIS PAGE INTENTIONALLY LEFT BLANK

INITIAL DISTRIBUTION LIST

1. Defense Technical Information Center
   Ft. Belvoir, Virginia

2. Dudley Knox Library
   Naval Postgraduate School
   Monterey, California

3. Physics Department
   Naval Postgraduate School
   Monterey, California

4. Professor Bruce Denardo
   Department of Physics
   Naval Postgraduate School
   Monterey, California

5. Professor Thomas Hofler
   Department of Physics
   Naval Postgraduate School
   Monterey, California

6. Kevin B. Smith
   Chair, Engineering Acoustics Academic Committee
   Naval Postgraduate School
   Monterey, California